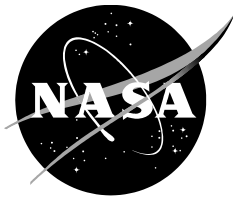


NASA/CR—2019–220062



Simulations of the Mars Helicopter Test Propeller in Hover Configuration at Martian Pressure and Air Density

*Lauren N. Wagner
Kentucky Space Grant Consortium
Ames Research Center, Moffett Field, California*

February 2019

NASA STI Program ... in Profile

Since its founding, NASA has been dedicated to the advancement of aeronautics and space science. The NASA scientific and technical information (STI) program plays a key part in helping NASA maintain this important role.

The NASA STI program operates under the auspices of the Agency Chief Information Officer. It collects, organizes, provides for archiving, and disseminates NASA's STI. The NASA STI program provides access to the NTRS Registered and its public interface, the NASA Technical Reports Server, thus providing one of the largest collections of aeronautical and space science STI in the world. Results are published in both non-NASA channels and by NASA in the NASA STI Report Series, which includes the following report types:

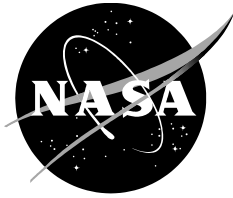
- **TECHNICAL PUBLICATION.** Reports of completed research or a major significant phase of research that present the results of NASA Programs and include extensive data or theoretical analysis. Includes compilations of significant scientific and technical data and information deemed to be of continuing reference value. NASA counterpart of peer-reviewed formal professional papers but has less stringent limitations on manuscript length and extent of graphic presentations.
- **TECHNICAL MEMORANDUM.** Scientific and technical findings that are preliminary or of specialized interest, e.g., quick release reports, working papers, and bibliographies that contain minimal annotation. Does not contain extensive analysis.
- **CONTRACTOR REPORT.** Scientific and technical findings by NASA-sponsored contractors and grantees.
- **CONFERENCE PUBLICATION.** Collected papers from scientific and technical conferences, symposia, seminars, or other meetings sponsored or co-sponsored by NASA.
- **SPECIAL PUBLICATION.** Scientific, technical, or historical information from NASA programs, projects, and missions, often concerned with subjects having substantial public interest.
- **TECHNICAL TRANSLATION.** English-language translations of foreign scientific and technical material pertinent to NASA's mission.

Specialized services also include organizing and publishing research results, distributing specialized research announcements and feeds, providing information desk and personal search support, and enabling data exchange services.

For more information about the NASA STI program, see the following:

- Access the NASA STI program home page at <http://www.sti.nasa.gov>
- E-mail your question to help@sti.nasa.gov
- Phone the NASA STI Information Desk at 757-864-9658
- Write to:
NASA STI Information Desk
Mail Stop 148
NASA Langley Research Center
Hampton, VA 23681-2199

NASA/CR—2019–220062



Simulations of the Mars Helicopter Test Propeller in Hover Configuration at Martian Pressure and Air Density

*Lauren N. Wagner
Kentucky Space Grant Consortium
Ames Research Center, Moffett Field, California*

National Aeronautics and
Space Administration

*Ames Research Center
Moffett Field, CA 94035-1000*

February 2019

ACKNOWLEDGMENTS

Special thanks to Witold Koning, without whose guidance and resources this project would not have been possible. Thank you for answering all my questions and trying to help with all my ridiculous RotCFD problems. Additional acknowledgments go to all the previous interns (Boles, McCoy, Johansson, and Koning) who provided the research that guided these results.

Another thank you goes to William Warmbrodt for his additional help and support, as well as to the NASA Kentucky Space Grant Consortium for funding this adventure. This internship has been a dream come true. And to the rest of the Aeromechanics Branch—a key part of my time here—thank you for all your support.

A special shout-out also goes to my Simulations team—Jesse Trujillo, Andrew Eskeldson, Joshua Walker-Ford, Michael May, Keiko Nagami, Victoria Cain, Kristen Anderson, Adam Bouma, and Jason Cornelius—for the silly jokes, pizza, midday breaks, and infinite help throughout this project. I definitely would not have made it through without you guys.

Available from:

NASA STI Support Services
Mail Stop 148
NASA Langley Research Center
Hampton, VA 23681-2199
757-864-9658

National Technical Information Service
5301 Shawnee Road
Alexandria, VA 22312
info@ntis.gov
703-605-6000

This report is also available in electronic form at
<http://ntrs.nasa.gov/>

TABLE OF CONTENTS

LIST OF FIGURES	iv
LIST OF TABLES	vii
NOMENCLATURE	viii
SUMMARY	1
INTRODUCTION	1
APPROACH	2
1. RotCFD Description and Background	2
2. Prior Work Performed.....	2
METHODS	3
1. 1013-mbar Setup.....	4
2. Grid Study.....	4
3. N242 Modeling	5
4. 14-mbar Setup.....	6
OBJECTIVES	10
RESULTS	11
1. Interpreting the Data	11
2. 1013-mbar and Grid Study Results.....	11
3. 14-mbar Results	14
CONCLUSIONS.....	16
FUTURE WORK.....	17
REFERENCES	18
APPENDIX A: RAW DATA	19
APPENDIX B: PREVIOUS DATA	25
APPENDIX C: ROTCFD RESULTS.....	29

LIST OF FIGURES

Figure 1.	MH mockup.	2
Figure 2.	Test propeller and stand setup.....	2
Figure 3.	1-Stack model.	3
Figure 4.	2-Stack model.	3
Figure 5.	Test stand and blast shields model.....	4
Figure 6.	Isolated rotor gridding.....	4
Figure 7.	PAL blueprint with dimensions.	5
Figure 8.	SOLIDWORKS drawing of PAL.	6
Figure 9.	Isolated rotor gridding.....	7
Figure 10.	N242 wall gridding.	7
Figure 11.	Stand and blast shields gridding.	8
Figure 12.	Full facility gridding.	8
Figure 13.	Maximum velocity setup gridding.	9
Figure 14.	Laser Lab gridding.	10
Figure 15.	Graph of 1-Stack relationships between 3,000-RPM data and previous data (Koning, Boles).....	12
Figure 16.	Graph of 2-Stack relationships between 3000-RPM data and previous experimental data (Boles).	13
Figure 17.	Flow with recirculation and movement around stand.....	15
Figure 18.	Sample flows for isolated run.	15
Figure 19.	Recirculation of flow in Laser Lab setup.....	16
Figure C1.	1013-mbar 1-Stack test 1 isol AGR gridding.	29
Figure C2.	1013-mbar 1-Stack test 1 isol residuals graph.	29
Figure C3.	1013-mbar 1-Stack test 1 isol CT graph.	30
Figure C4.	1013-mbar 1-Stack test 1 isol thrust graph.	30
Figure C5.	1013-mbar 1-Stack test 1 isol total power graph.	31
Figure C6.	1013-mbar 1-Stack test 1 isol velocity visualization.	31
Figure C7.	1013-mbar 1-Stack test 2 isol thrust.	32
Figure C8.	1013-mbar 1-Stack test 2 isol velocity.....	32
Figure C9.	1013-mbar 1-Stack test 6 isol thrust.	33
Figure C10.	1013-mbar 1-Stack test 6 isol velocity.....	33

LIST OF FIGURES (continued)

Figure C11. 1013-mbar 1-Stack test 7 isol thrust.	34
Figure C12. 1013-mbar 1-Stack test 7 isol velocity.	34
Figure C13. 1013-mbar 1-Stack test 8 isol thrust.	35
Figure C14. 1013-mbar 1-Stack test 8 isol velocity.	35
Figure C15. 1013-mbar 1-Stack test 9 isol thrust.	36
Figure C16. 1013-mbar 1-Stack test 10 full thrust.	36
Figure C17. 1013-mbar 1-Stack test 10 velocity.	37
Figure C18. 1013-mbar 2-Stack test 1 isol residual.	37
Figure C19. 1013-mbar 2-Stack test 1 isol CT.	38
Figure C20. 1013-mbar 2-Stack test 1 isol thrust.	38
Figure C21. 1013-mbar 2-Stack test 1 isol total power.	39
Figure C22. 1013-mbar 2-Stack test 1 isol velocity.	39
Figure C23. 1013-mbar 2-Stack test 2 isol thrust.	40
Figure C24. 1013-mbar 2-Stack test 2 isol velocity.	40
Figure C25. 1013-mbar 2-Stack test 3 isol thrust.	41
Figure C26. 1013-mbar 2-Stack test 3 isol thrust.	41
Figure C27. 1013-mbar 2-Stack test 3 isol velocity.	42
Figure C28. 1013-mbar 2-Stack test 4 isol thrust.	42
Figure C29. 1013-mbar 2-Stack test 4 isol velocity.	43
Figure C30. 1013-mbar 2-Stack test 5 isol thrust.	43
Figure C31. 1013-mbar 2-Stack test 6 isol thrust.	44
Figure C32. 14-mbar 1-Stack test 1 isol residual.	44
Figure C33. 14-mbar 1-Stack test 1 isol CT.	45
Figure C34. 14-mbar 1-Stack test 1 isol thrust.	45
Figure C35. 14-mbar 1-Stack test 1 isol total power.	46
Figure C36. 14-mbar 1-Stack test 2 N242 thrust.	46
Figure C37. 14-mbar 1-Stack test 2 N242 velocity.	47
Figure C38. 14-mbar 1-Stack test 7 full thrust.	47
Figure C39. 14-mbar 1-Stack test 7 full velocity.	48
Figure C40. 14-mbar 1-Stack test 8 full thrust.	48
Figure C41. 14-mbar 1-Stack test 8 full velocity.	49

LIST OF FIGURES (concluded)

Figure C42. 14-mbar 1-Stack test 9 full thrust.	49
Figure C43. 14-mbar 1-Stack test 9 full velocity.....	50
Figure C44. 14-mbar 1-Stack test 10 full thrust.	50
Figure C45. 14-mbar 1-Stack test 10 full total power.	51
Figure C46. 14-mbar 1-Stack test 10 full velocities.	51
Figure C47. 14-mbar 1-Stack test 12 Laser Lab thrust.	52
Figure C48. 14-mbar 1-Stack test 12 Laser Lab total power.	52
Figure C49. 14-mbar 1-Stack test 12 Laser Lab velocity.	53
Figure C50. 14-mbar 1-Stack test 13 max velocity thrust.	53
Figure C51. 14-mbar 1-Stack test 13 max velocity visualization.	54
Figure C52. 14-mbar 1-Stack test 14 max velocity thrust.	54
Figure C53. 14-mbar 1-Stack test 14 max velocity total power.	55
Figure C54. 14-mbar 1-Stack test 14 max velocity visualizations.	55
Figure C55. 14-mbar 2-Stack test 5 full residual.	56
Figure C56. 14-mbar 2-Stack test 5 full CT.	56
Figure C57. 14-mbar 2-Stack test 5 full thrust.	57
Figure C58. 14-mbar 2-Stack test 5 full total power.	57
Figure C59. 14-mbar 2-Stack test 5 full velocity.....	58
Figure C60. 14-mbar 2-Stack test 6 N242 thrust.	58
Figure C61. 14-mbar 2-Stack test 6 N242 velocity.	59
Figure C62. 14-mbar 2-Stack test 8 max velocity thrust.	59
Figure C63. 14-mbar 2-Stack test 8 max velocity visualization.	60
Figure C64. 14-mbar 2-Stack test 9 isol thrust.	60
Figure C65. 14-mbar 2-Stack test 9 isol velocity.	61

LIST OF TABLES

Table 1. Simulation Conditions for Two Setups	3
Table 2. Boundary Conditions for PAL	6
Table 3. Wall Conditions Used in Maximum Velocity Simulation	9
Table 4. Boundary Conditions for Laser Lab Setup.....	10
Table 5. 1-Stack 1013-mbar Run Data	11
Table 6. 2-Stack 1013-mbar Results	13
Table 7. 14-mbar Testing Run Results	14
Table 8. Averaged Stand Effects	15
Table A1. Raw Data for 1013-mbar 1-Stack Runs	19
Table A2. Raw Data for 1013-mbar 2-Stack Runs	20
Table A3. Raw Data for 14-mbar 1-Stack Runs	21
Table A4. Raw Data for 14-mbar 2-Stack Runs	23
Table B1. 1013-mbar 1-Stack AGR Sweep Data (Koning)	25
Table B2. 1013-mbar 1-Stack NAGR Sweep Data (Koning).....	25
Table B3. 1013-mbar 1-Stack Experimental Sweep Data (Boles)	25
Table B4. 1013-mbar 2-Stack Casing Sweep Data (McCoy).....	26
Table B5. 1013-mbar 2-Stack No Casing Sweep Data (McCoy).....	26
Table B6. 1013-mbar 2-Stack Experimental Sweep Data (Boles)	26
Table B7. 1013-mbar 2-Stack Simulation Data (Koning).....	27
Table B8. 1013-mbar 2-Stack Simulation Sweep (Johannson).....	27

NOMENCLATURE

1-Stack	one-propeller setup, two blades
2-Stack	two-propeller setup, four blades
AGR	adaptive grid refinement
CAD	computer aided design
CFD	computational fluid dynamics
CT	coefficient of thrust
GPU	graphics processing unit
GUI	graphical user interface
MARSWIT	Martian Surface Wind Tunnel
mbar	millibars, unit of pressure
MH	Mars Helicopter
N	Newtons; unit of force
(N)AGR	(non)-adaptive grid refinement
N242	location of the PAL and MARSWIT at Ames Research Center
PAL	Planetary Aeolian Laboratory
RANS	Reynolds-Averaged Navier-Stokes
RotCFD	Rotorcraft Computation Fluid Dynamics
RPM	rotations per minute

Simulations of the Mars Helicopter Test Propeller in Hover Configuration at Martian Pressure and Air Density

Lauren Wagner*

Ames Research Center

SUMMARY

In order to properly validate experimental data, a theoretical model must be generated and converge with the results. Providing possible results for future testing can help experimenters better understand the results they are getting. Certain effects cannot be shown during experimentation and must therefore be quantified through other means. A rotor blade similar to that of the Mars Helicopter (MH) is currently being tested in the Martian Surface Wind Tunnel (MARSWIT) in the Planetary Aeolian Laboratory (PAL) at NASA Ames Research Center, which can reach a pressure and air density similar to that of the Martian atmosphere. The test propeller was analyzed in a computational fluid dynamics (CFD) solver. The propeller blades were previously modeled, and were simulated in the full experimental setup, which includes the blast shields, rotor stand, and tunnel walls, to thoroughly generate the effects of the true testing conditions. Simulations were run using both an isolated hover condition and with the full setup, and results for thrust and total power were quantified. The data generated was used to quantify the impact of the facility on the propeller. These calculations will ultimately be used to help separate these effects from the actual thrust that the propeller will generate, thus making the data more accurate.

INTRODUCTION

A propeller meant to emulate the Mars Helicopter (MH) (Fig. 1) is currently being tested in the Martian Surface Wind Tunnel (MARSWIT) in the Planetary Aeolian Laboratory (PAL) at NASA Ames Research Center. The pressure chamber of the PAL in Building N242 can reach the pressure and air density similar to the conditions found on Mars. N242 and PAL are used synonymously from here on. The goal of this testing is to emulate how the MH will function while on Mars. Hover is one of the many configurations that will be tested. In order to perform hover testing, however, the propeller must be stacked onto a test stand (Fig. 2), with blast shields to protect the PAL in case of failure; these additions will have an effect on how the propeller operates. In addition, the walls of N242 could cause recirculation that would not be found when the MH is operating in its true conditions. Therefore, simulations need to be run before testing can be performed in order to quantify how the experimental setup will affect the test results.

* NASA Kentucky Space Grant Consortium, Lexington, KY 40506-0108.



Figure 1. MH mockup.



Figure 2. Test propeller and stand setup.

APPROACH

This project involved the use of a CFD program. Rotorcraft Computation Fluid Dynamics (RotCFD), a mid-fidelity program capable of handling moderately large grid generation, was chosen. The program can handle the wide range of conditions needed for the project. Propeller files were generated previously using the program C81Gen, and facility geometry was created using the computer aided design (CAD) software, SOLIDWORKS[®]. Previous data from past tests and simulations were also used to confirm the validity of the results. These tasks were performed on a computer with mid-level specifications, and the graphics processing unit (GPU) could handle a maximum cell count of 1.3 million cells, which was the significant limiting factor of the project. Data was stored and analyzed using Excel, with graphs coming from both Excel and RotCFD.

1. RotCFD Description and Background

RotCFD was the main program used for the project in this report. It was developed specifically for use by NASA and the Army but is freely available to all who can use it. RotCFD can analyze both bodies and rotors, and calculate flow and forces acting on these parts. It runs through the use of Reynolds-Averaged Navier-Stokes (RANS) equations. The graphical user interface (GUI) is specifically designed to be easy to use and understand. A short learning curve was built into the timeline for the project.

2. Prior Work Performed

Work has been performed by previous aeromechanics interns. Their work documents results from other simulations at a variety of tip speeds and grid setups. The data they generated serves as a starting and comparison point for hover testing at 3,000 RPM. A majority of the data was placed into a single Excel spreadsheet (with any missing information copied over from previous final papers) that contained both experimental and simulation data.

Since the prior data came from a variety of sources and setups, certain generalizations were made to allow for that data to be used for comparison to the simulation data. First, the results had to be proven to converge with each other before proceeding with other changes. Thus, both experimental and simulation data can be used to confirm the simulation results.

METHODS

A variety of programs were used for this project; RotCFD was the main program used for simulating the MH. Files were provided that contained models of the propeller(s), test stand, and blast shields. There were two separate airfoil tables provided, one for Earth simulation and one for Martian simulation, as it was determined that the Reynolds number effects in Mars simulations are substantial. These files also contained an Excel spreadsheet that listed all the data from previous experimental tests and simulations. Using the given data, simulations could be run at Earth and Martian pressures (see Table 1) and compared to the previous data to confirm the accuracy of the results.

Two different hover configurations of blades were used for simulation: 1-Stack and 2-Stack blade setups, thrusting upward (Figs. 3, 4). All testing was performed at 3,000 RPM. All simulations were run in steady blade condition, which led to a loss of the 90-degree phase angle between the blades in a 2-Stack. In addition, a variety of facility settings were tested: isolated, with N242 walls, with the test stand and blast shields (Fig. 5), and with all facility conditions. The program SOLIDWORKS was used to generate a model of the wall geometries of N242. Additional setups were later used to attempt generating recirculation. These setups allowed for an understanding of how the different facilities affected the outputs generated, most notably the thrust. Simulations were also run for a variety of time lengths and time steps, to view how the outputs changed with different amounts of times and accuracy.

Table 1. Simulation Conditions for Two Setups

Condition	Earth	Mars
Pressure (mbar)	1013	14
Density (kg/m ³)	1.225	0.01612
Tip Speed (m/s)	160.5	160.5
Propeller Length (m)	1.022	1.022
Airfoil Table	1013-mbar Table	7-mbar Table

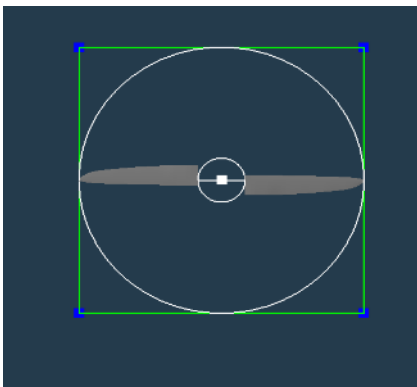


Figure 3. 1-Stack model.

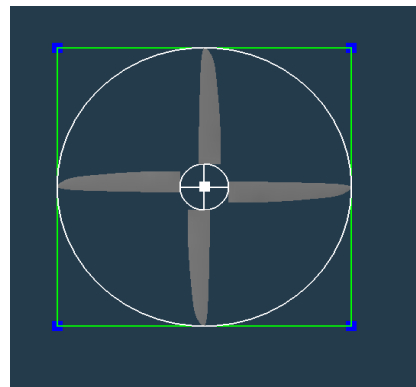


Figure 4. 2-Stack model.



Figure 5. Test stand and blast shields model.

1. 1013-mbar Setup

The validity of simulations was first confirmed using previous testing data. Simulations and experiments have been performed by previous interns, at a variety of blade speeds. These sweeps create linear relationships that can be used to confirm the results of simulations at 3,000 RPM. Most these simulations used an isolated run setup, but some were run using facility effects in order to verify the values generated in experimental data. Both 1-Stack and 2-Stack testing were performed. The simulations were allowed to run until thrust and residual values converged, usually taking around 0.1 seconds of simulation time, or 10 rotations.

2. Grid Study

Once the validity of the simulations was proven through 1013-mbar isolated rotor simulation and comparison, this type of simulation could be used to determine what grid changes could be made (Fig. 6). Multiple simulations were run while changing grid and time settings in RotCFD, to see how quickly a simulation could be run while still aligning with the results generated in the first steps of this project. The first step taken to speed up the simulation was changing the propeller state to steady and, secondly, turning off adaptive grid refinement (AGR). These two steps

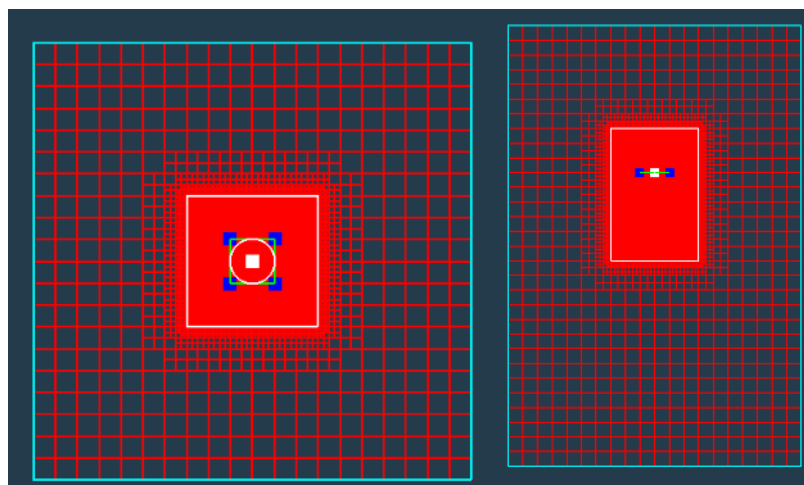


Figure 6. Isolated rotor gridding.

drastically increase the amount of time needed to run a simulation. Unsteady propellers take more measurements per rotation, instead of taking the summation of work done by the propeller disk. AGR makes adjustments to the grid with each time step, making it more accurate, but requiring a certain amount of simulation run time to be dedicated to changing the grid. For each run, one change was made to the simulation, with thrust, power, and coefficient of thrust (CT) averages taken once the values converged. These averages could then be compared to determine whether or not the change impacted the results of the simulation.

3. N242 Modeling

The geometries of the walls in N242 needed to be modeled in order to accurately characterize the facility effects for this project. Blueprints of the building were obtained (Fig. 7), and the dimensions were used to recreate the walls using the CAD program SOLIDWORKS (Fig. 8). A solid body that would fill the full boundary spacing was chosen to make it easier for RotCFD to generate a grid. The chamber was converted to SI units to maintain consistency and entered into RotCFD.

The boundary conditions listed in Table 2 were used for a majority of the 14-mbar testing, as they were very close to the dimensions of the PAL. The only adjustment was making the ceiling height 20 meters instead of 30 meters, in order to get a fine enough gridding.

The PAL geometry provided a large challenge for grid generation. The odd angles of the walls made gridding difficult because the cells could not align tightly to the walls, like they could with the blast shields and test stand. This was overcome by making the refinement level of the walls much lower than that of the test stand and blast shields, typically a 4:6 ratio.

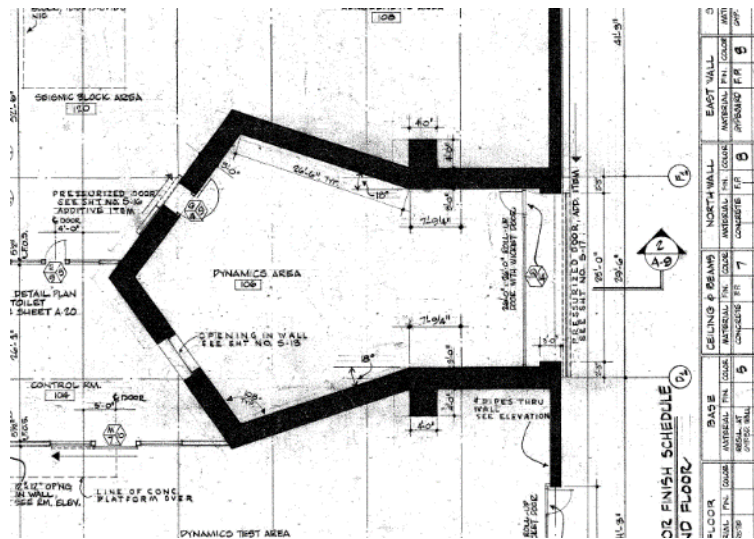


Figure 7. PAL blueprint with dimensions.

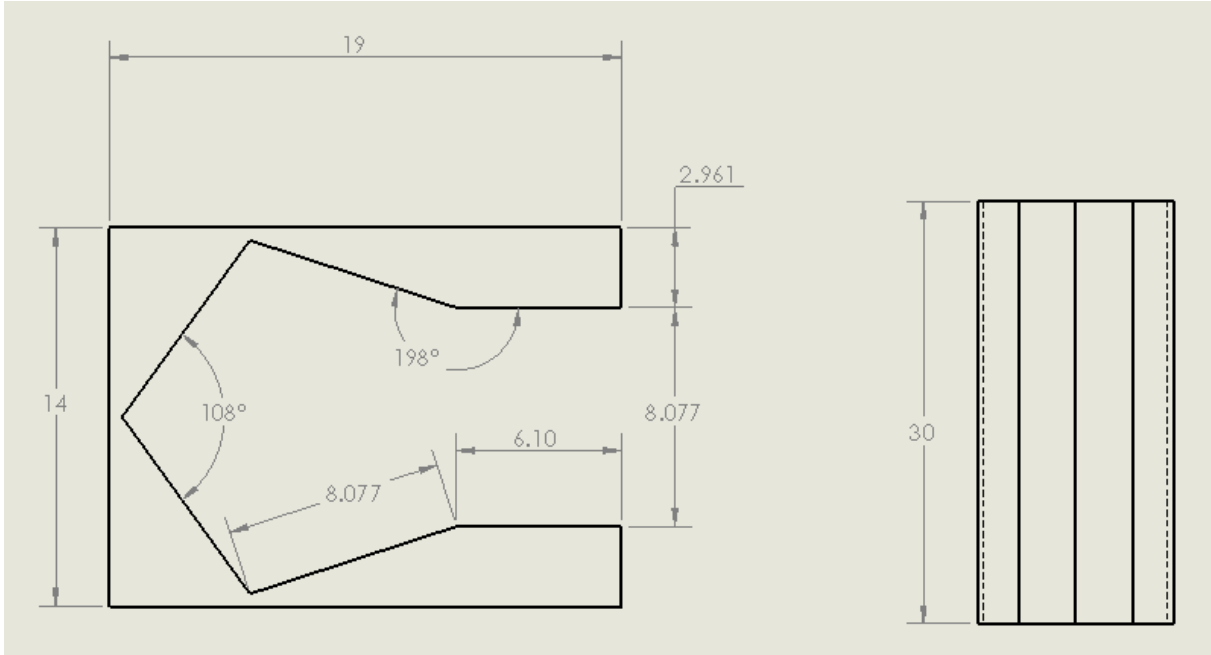


Figure 8. SOLIDWORKS drawing of PAL.

Table 2. Boundary Conditions for PAL

Plane	Dimension (m)
X-Min	-6.5
X-Max	12.5
Y-Min	-7.0
Y-Max	7.0
Z-Min	0
Z-Max	20

4. 14-mbar Setup

Once all the steps above were completed, simulation at 14 mbar could be completed. Four setups with varying geometries were created: isolated rotor, N242 walls with propeller, test stand and blast shields with propeller, and all aspects combined. Simulations were run in both 1- and 2-Stack, resulting in eight different testing setups. Figures 9 through 12 below are 1-Stack setups, as there is only a minimal difference for the rotor gridding for 2-Stack. This allowed for an understanding of how the different facility conditions would affect the output values. All testing took place in a boundary setup that was very close to the wall geometry, so that even when the walls were not physically there, the flow was still similar. The maximum cell size was 0.5 meters for almost all runs. Many of the same grid and time adaptations were made to these simulations as were made in the grid study. In addition, Larry Young provided advice on how to best reach recirculation results, and these changes were added to later tests. Boundary refinement on the floor and ceiling was also used in later simulations, in order to provide more accurate flow

understanding in these spots. Simulations were run for a variety of times, in order to better understand when recirculation would occur. For each run, CT, thrust, and power were averaged, with multiple simulations of the same setup averaged later. This gave a clearer reading of the simulation outputs than graphing.

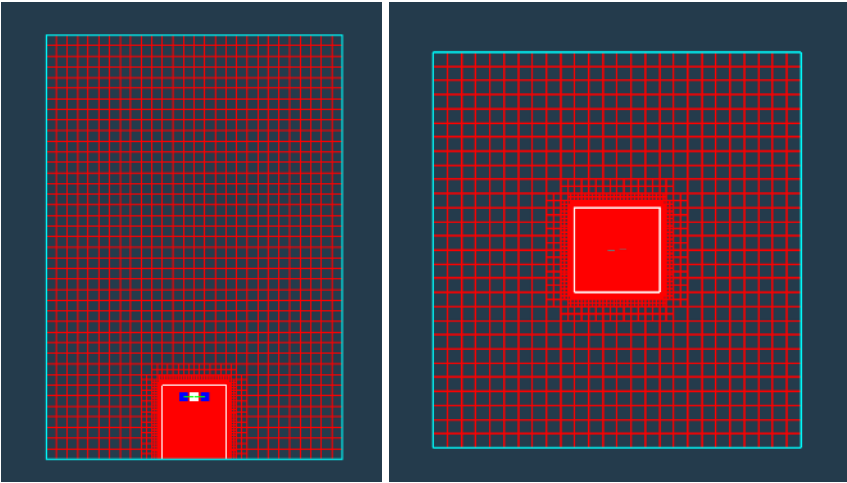


Figure 9. Isolated rotor gridding.

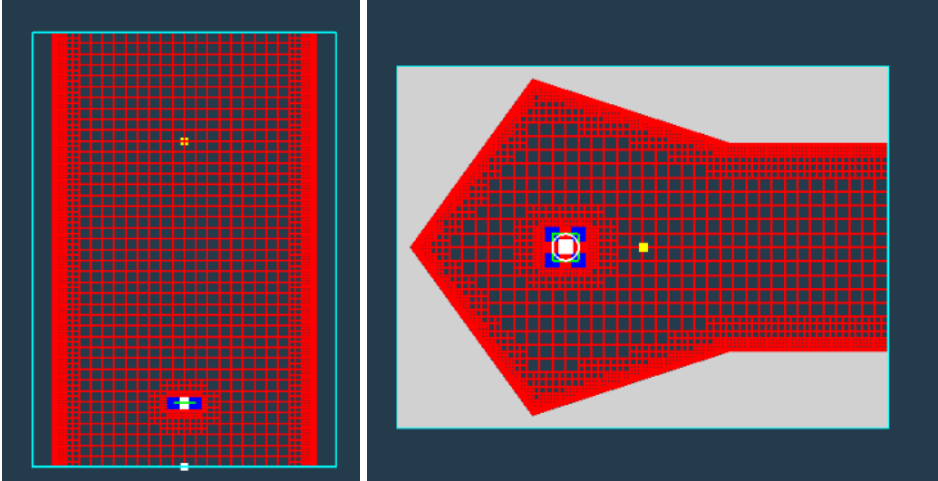


Figure 10. N242 wall gridding.

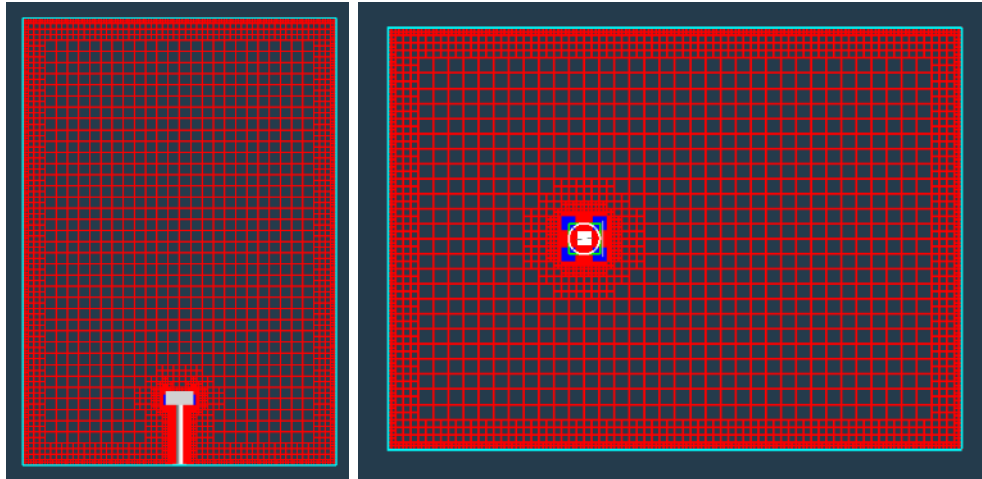


Figure 11. Stand and blast shields gridding.

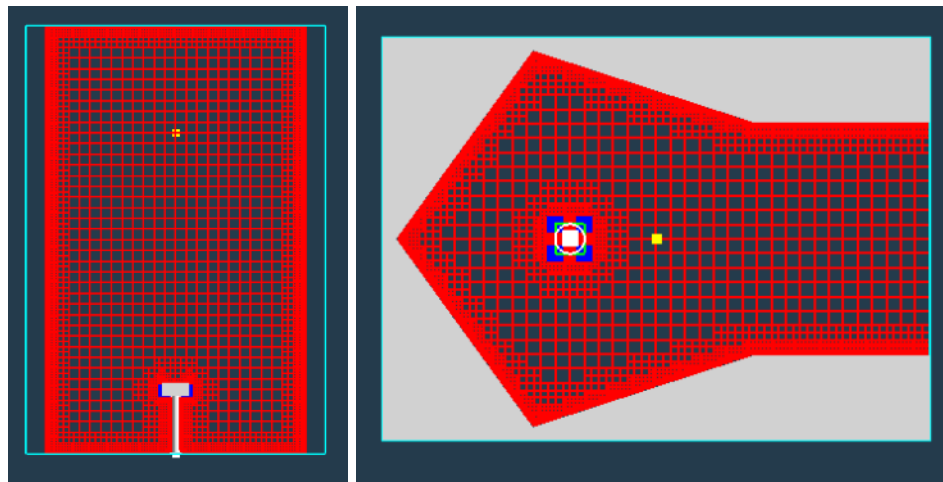


Figure 12. Full facility gridding.

i. Shift From 7 mbar

Simulation was initially set to use 7 mbar and equivalent density to create Martian conditions. The assumption was made that similar pressure would be achievable when performing hover testing. This led to shifting the simulations to 14-mbar pressure, and equivalent density as well, in order to more accurately understand the true testing that would occur. Though testing at 7 mbar may be possible in hover configuration, 14 mbar is a known, working experimental condition.

This led to some issues in using propeller models and comparing to past results. Airfoil tables were generated specifically for 7-mbar simulation. The assumption was made that these tables would provide a close enough model to the one needed for 14 mbar, allowing for its use because of the moderate difference in expected Reynolds number effects. This comparison also carries over into data analysis for past simulations at 7 mbar. While the data cannot be directly

compared, it provides a reference point for where the 14-mbar data should be, although the changes should be minimal. For example, when there was an error in the density input, the thrust values were incorrect. This led to the incorrect value being discovered sooner and changed.

ii. Additional Setups

In later testing, different setups were used in an attempt to better understand recirculation. A velocity equivalent to the maximum velocity generated by the propeller was generated to come from the ceiling to flow down to the propeller, in order to create a “worst-case scenario” for the maximum amount of recirculation speed the blade could experience (Fig. 13). A maximum velocity value was acquired from recirculation attempts, and the condition was applied in one case to all walls except the ground, and only to the ceiling in another case. This testing used the stand and blast shields setup, with the wall condition changed from 0 to 17.8 m/s velocity as the only adjustment (see Table 3). All other conditions remained the same as the normal full setup.

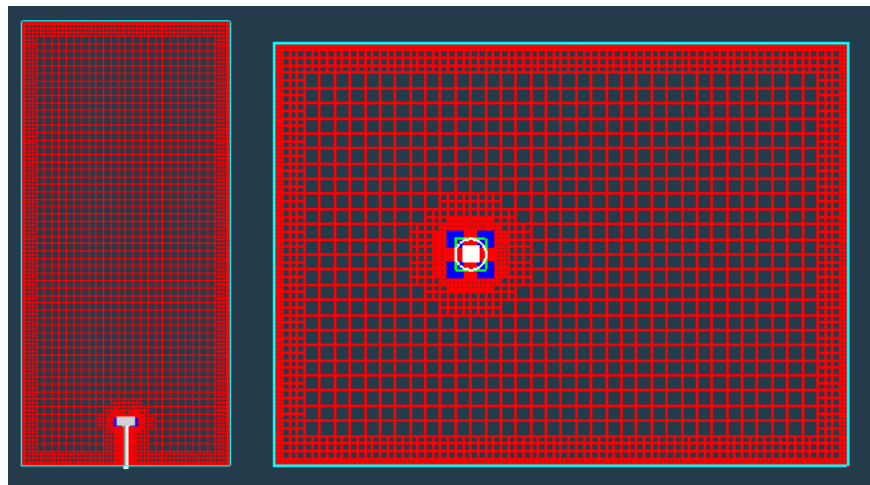


Figure 13. Maximum velocity setup gridding.

Table 3. Wall Conditions Used in Maximum Velocity Simulation

Wall	1-Stack (Setup 1)	1-Stack (Setup 2)	2-Stack
X-Min	-17.8 m/s	0	-21.4 m/s
X-Max	-17.8 m/s	0	-21.4 m/s
Y-Min	-17.8 m/s	0	-21.4 m/s
Y-Max	-17.8 m/s	0	-21.4 m/s
Z-Min	Outflow	Outflow	Outflow
Z-Max	-17.8 m/s	-17.8 m/s	-21.4 m/s

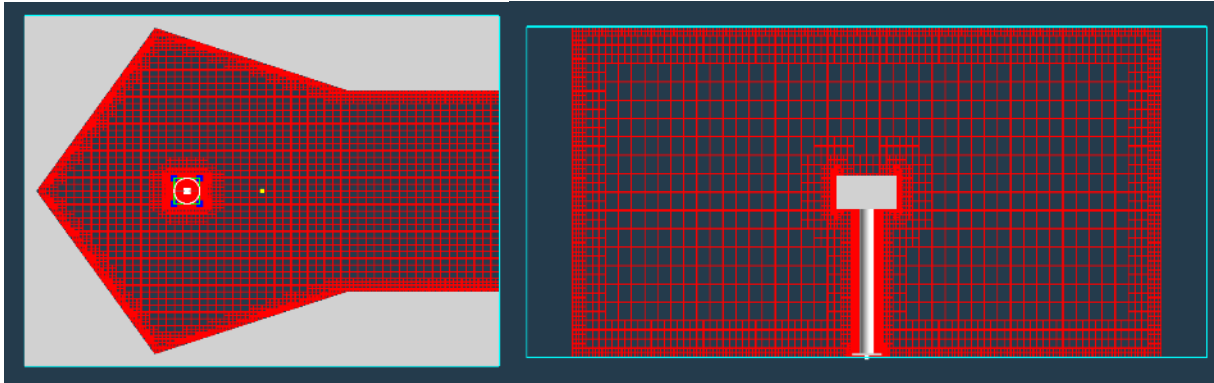


Figure 14. Laser Lab gridding.

Table 4. Boundary Conditions for Laser Lab Setup

Wall	Boundary (m)
X-Min	-6.5
X-Max	12.5
Y-Min	-7
Y-Max	7
Z-Min	0
Z-Max	6

Another additional setup involved using a wall height similar to the one found in the Laser Lab (Fig. 14 and Table 4). The ceiling, at around 6 meters, is much shorter in that building, which provided two advantages: the air did not have to travel as far up the wall in order to reflect off the ceiling, and denser gridding could be used, which would give more accurate results. The geometry was used to visualize how the flow would bounce off the oddly shaped walls.

OBJECTIVES

The overall goal of this project was to predict the behavior of the test propeller while operating under Martian conditions in hover configuration. The first step to meeting this goal involved confirming results of the simulation and improving the amount of time taken to generate accurate results. This involved running simulations at Earth pressure and comparing results to experimental data taken by others. Once the data was confirmed, various changes were made to the grid in order to improve the amount of time needed to run the simulation. This meant running simulations with various changes made to the grid conditions, and comparing them again to the experimental data.

Once the results of the grid changes were confirmed, testing was shifted to Martian conditions. The grid changes used on the testing at Earth conditions were applied to the Mars simulations, and the various setups were created. Simulations were then run with the intent of understanding the facility effects, with specific interest placed on the potential for recirculation. These results were again confirmed using previous testing and simulation data, and any effects were quantified.

RESULTS

1. Interpreting the Data

While collecting data throughout the project, a common strategy for interpreting the data involved taking a subsection of the data where it was consistent. In every simulation, the data started out by spiking up, before falling down to a constant value, as is common with programs. Simulations were run to convergence, where the values became near-constant. The data would also occasionally spike toward the end, as the total mass residual grew and the simulation began to diverge. Therefore, it was reasonable to examine the data where the values were most likely correct, where there were no large residuals.

Some tests were deliberately excluded from this report because of incorrect results. However, they were left in the testing order (see Appendix C), in order to describe why they failed, as a note to future workers on this project.

2. 1013-mbar and Grid Study Results

Most values generated during the grid study proved the validity of simulations for 1013 mbar (see Table 5). A single AGR run was performed for confirmation with the variety of previous results. The simulation showed strong validity. A linear relationship exists between thrust and RPM^2 , with the 3,000-RPM simulation aligned to those results. The data was tested for both 1- and 2-Stack setups, in the isolated and full-setup configurations. This confirmed that the values would be accurate in an experimental setup.

With the expected values for 3,000-RPM simulations at Earth conditions determined, changes could be made to the simulation to determine how quickly the simulation could be run while maintaining accuracy. Changes were implemented one at a time, and mostly involved making the grid less dense in order to comply with the limitations of the graphics card. A majority of the changes made resulted in faster runs with equivalent data.

Table 5. 1-Stack 1013-mbar Run Data

1-Stack	RESULTS	Cells	Time Steps	Sim Time (s)	Comment	CT	Thrust (N)	Total Power (W)
ISOLATED	Test 1	1681192	7200	2	AGR (BASE)	0.01249	325	6211
	Test 9	1681192	7200	2	FULL RUN	0.01254	324.3	6184.9
	Test 4	1681192	7200	2	NAGR	0.012489	323.9	6244.8
	Test 6	866624	5000	2	Grid/ Time	0.01249	323.03	6246.7
	Test 7	866624	5000	2	OpenCL	0.0126	325.9	6230.9
	Test 8	866624	500	2	Short	0.0127	328.3	6351
	AVERAGE					0.0125515	325.1	6244.9
FULL	Test 10	1323928	5000	50		0.0113407	293.19	6458.4

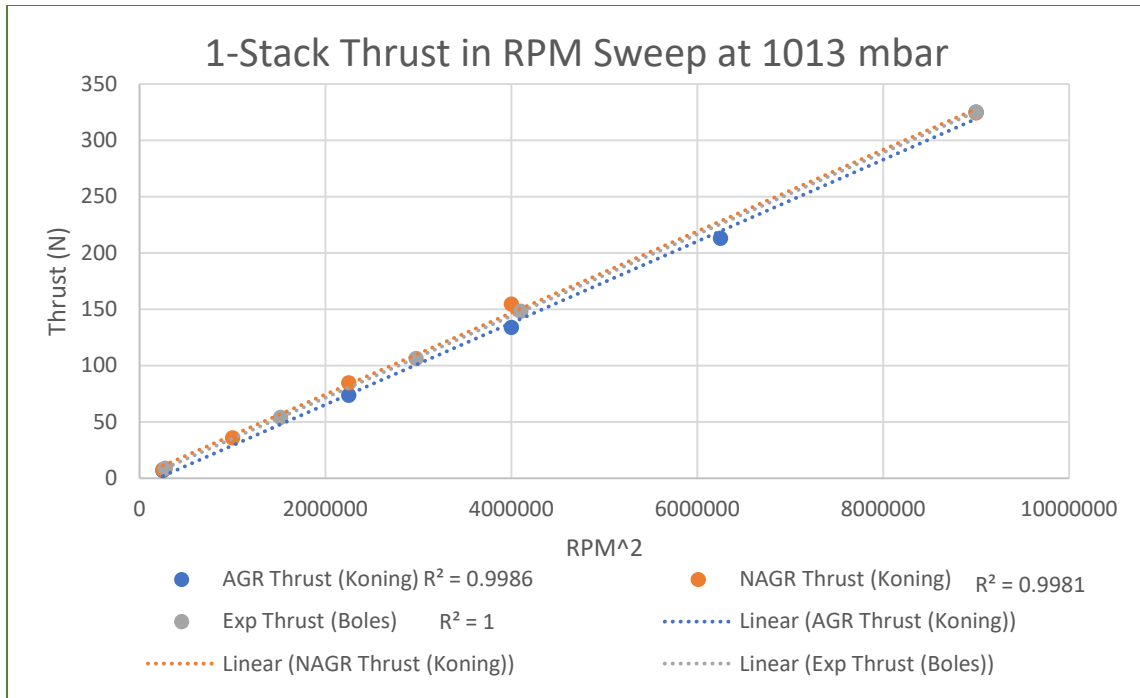


Figure 15. Graph of 1-Stack relationships between 3,000-RPM data and previous data (Koning, Boles).

Previous sweep simulations had been run for 1-Stack simulations, leading to the creation of multiple line fits (Fig. 15). AGR/non-adaptive grid refinement (NAGR) refer to simulation runs, while Exp references experimental testing. The 3,000-RPM simulations align very well with all previous data, with high R^2 values. The average value of all the runs was used for the experimental data point, and has the highest R^2 value, indicating accuracy in the grid study performed.

Fewer runs were performed for 2-Stack simulations (see Table 6); many of the changes were well documented in the 1-Stack, so there was less trial and error in cases, leading to fewer, less useful simulations. The ultimate factors that seemed to influence the length of the simulation were the two changes previously mentioned, NAGR and steady blade. Another significant improvement in time came from switching the program control from OpenMP to OpenCL. This allowed for significant time improvements with the same results, but was the cause of the limit in the number of cells, as the simulation fails if there is not enough graphics card memory. Adjustments to time were made, but later were determined case by case, as more bodies required a higher ratio of time steps per simulation second, while isolated runs would successfully converge at a 1:1 ratio of time step to simulation second. Grid refinements were also ultimately determined case by case, through trial and error, but ran best around the 1.3 million cell limit, which seemed to maximize accuracy of results while minimizing errors. Grids with significantly more cells took far too long to generate, while smaller grids would diverge quickly. Therefore, certain changes could be made outright, while grid and time changes can be closely estimated, but ultimately needed to be determined on a case-by-case basis.

Table 6. 2-Stack 1013-mbar Results

2-Stack	RESULTS	Cells	Time Steps	Sim Time (s)	Comment	CT	Thrust (N)	Total Power (W)
ISOLATED	Test 1	1737696	7200	2	BASE	0.020551	532.36	12305.7
	Test 3	1737696	7200	2	BASE	0.020756	536.6	12262.5
	Test 2	1737696	7200	2	Phase	0.02056	531.57	11712.3
	Test 4	1015296	7200	2	Grid	0.020886	539.6	12111
	Test 5	1737696	500	2	Short	0.02116	547	12248.4
	AVERAGE					0.0207826	537.426	12127.98
FULL	Test 6	1147884	7200	2		0.018297	473.1	12482.1

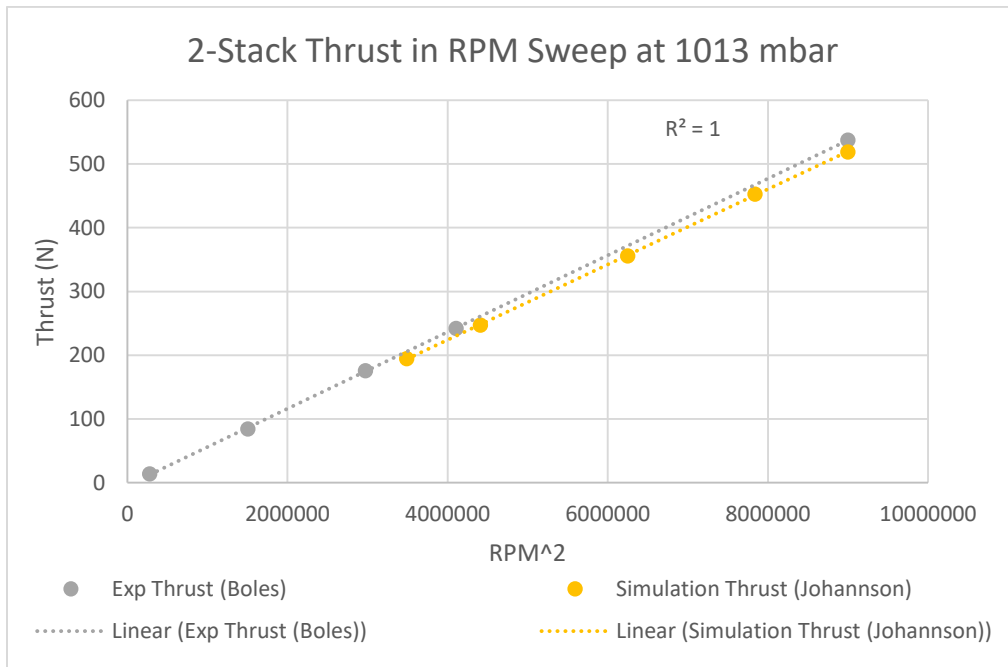


Figure 16. Graph of 2-Stack relationships between 3000-RPM data and previous experimental data (Boles).

Other previous data existed for 2-Stack runs, but they used a unique setup that did not provide as strong of a correlation (Fig. 16). Again, all values were averaged and used for the 3,000-RPM run, with high accuracy. Base runs refer to benchmark runs, with minimal changes to the gridding or time. Test 2 involved running a simulation with one blade left on unsteady, as a way of maintaining the phase delay that the actual propeller has in 2-Stack. Thus, the grid changes used for 1-Stack simulations can successfully be added to 2-Stack. These data points were also compared to simulations run previously at 3,000 RPM (see Appendix B). Many of the values were found to be slightly lower than the ones generated. However, this is most likely due to the use of unsteady blade, which has a higher accuracy. This issue was not as noticeable with one blade, but a two-blade setup has more interference and issues.

A run was also performed for both blade arrangements and full-facility effects, in order to examine how the stand affected values at Earth conditions. As seen above, there was a small drop in thrust and CT, around 11 percent for both runs and values, with minimal effect on total power consumption. This is logical, as the setup will obstruct some thrust, but it should not change the power output.

3. 14-mbar Results

Multiple runs were performed, again mainly using the 1-Stack for most of the trial and error, and carrying over significant changes to 2-Stack simulations (see Table 7). No simulations have previously been run for hover configuration at 14 mbar, so there is minimal old data to compare to. The same findings from 1013-mbar testing were used as a base point for how the flow should respond to the testing conditions.

Recirculation was not generated using a normal setup. Test 10 ran for 200 real-time seconds, and only made it halfway up the wall. However, there were slight differences noted in the stand (Fig. 17) and isolated runs (Fig. 18). These differences were also noted in runs at 1013 mbar. Based on the movement of the flow, it can also be assumed that the change is most heavily associated with the test stand as opposed to the blast shields. The flow is noticeably pushed outward by the stand, as opposed to the straight flow of an isolated run (see Table 8). The differences between isolated and full-setup runs were quantified.

Table 7. 14-mbar Testing Run Results

14 mbar								
1-Stack	RESULTS	Cells	Time Steps	Sim Time (s)	Comment	CT	Thrust (N)	Total Power (W)
ISOLATED	Test 1	1288000	7200	2		0.004969	1.69	67.5
N242	Test 2	915000	15000	15		0.004924	1.676	74.69
FULL	Test 7	1156000	20000	200	diverges early	0.00479	1.63	74.5
	Test 8	1091000	20000	200		0.00469	1.6	74.322
	Test 9	1091000	20000	200		0.00474	1.608	74.5
	Test 10	1305000	20000	200	BOUNDARY RF	0.00485	1.65	74.8
	AVERAGE					0.0047675	1.622	74.5305
VELOCITY	Test 13	1153746	5000	50	setup 1	0.002914	0.9915	66.373
	Test 14	1153746	5000	50	setup 2	0.002867	0.9756	66.08
	AVERAGE					0.0028905	0.98355	66.2265
LASER LAB	Test 12	901396	20000	200		0.004717	1.605	73.6
2-Stack	RESULTS	Cells	Time Steps	Sim Time (s)	Comment	CT	Thrust (N)	Total Power (W)
ISOLATED	Test 9	990044	2000	20		0.008412	2.8624	140.1
N242	Test 6	1129804	20000	200		0.008276	2.8137	139.137
FULL	Test 5	1212060	20000	200		0.007767	2.6313	138.064
VELOCITY	Test 8	1153749	5000	500	setup 1	0.004406	1.4992	119.842

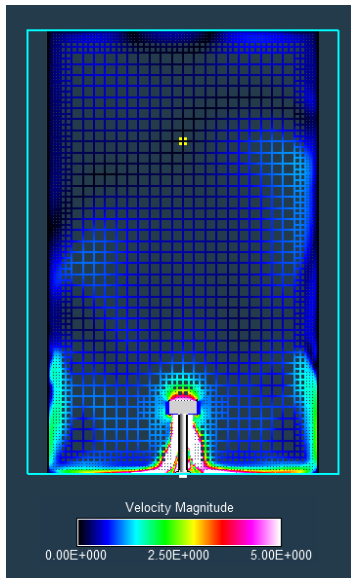


Figure 17. Flow with recirculation and movement around stand.

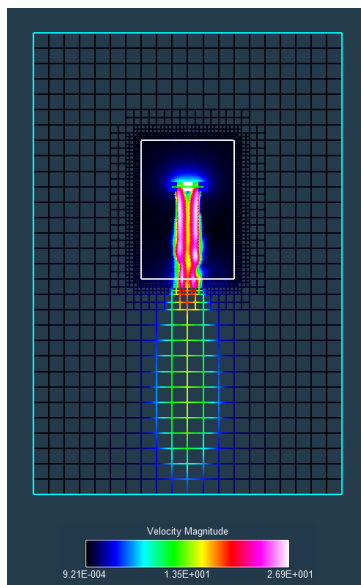


Figure 18. Sample flows for isolated run.

Table 8. Averaged Stand Effects

	Isolated T (N)	Stand T (N)	Difference (%)
1013 1-Stack	325.07	293.19	9.81
1013 2-Stack	537.4	473.1	11.97
14 1-Stack	1.69	1.622	4.02
14 2-Stack	2.862	2.631	8.07

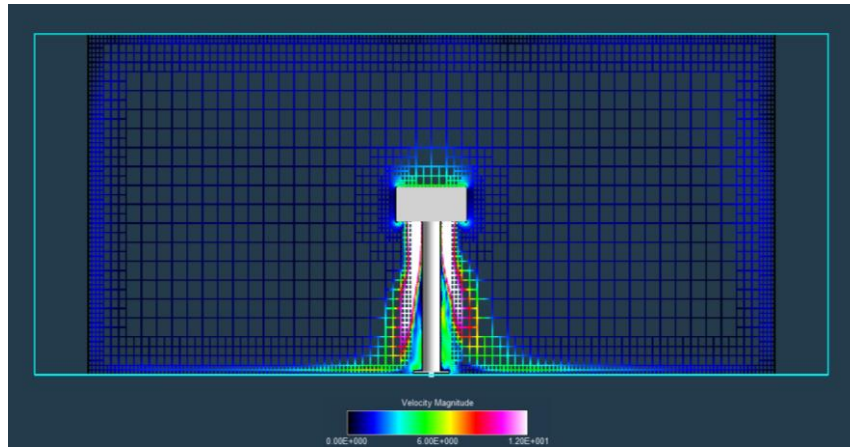


Figure 19. Recirculation of flow in Laser Lab setup.

This led to the use of two extra cases to “force” recirculation. The velocity was calculated from Test 10, and applied to the boundaries. Running with the velocity condition caused a reduction around 40 percent. When running with the Laser Lab setup (Fig. 19), the velocity only dropped an insignificant amount, as only a slower velocity flow recirculated, and ultimately had a very minimal impact on thrust and other values. Therefore, the N242 walls will not noticeably affect experimental runs.

Results with a similar trend were generated for 2-Stack simulations. The isolated and N242 runs had similar results, with a small change in the full setup as a result of the blast shields and test stand blocking some thrust. Running with the velocity condition caused a drop of approximately 43 percent. This is a worst-case scenario, where the fastest wind speed reaches the propeller from the top. The value is larger in 2-Stack because of the increased velocity generated by the use of two blades.

CONCLUSIONS

Overall, facility effects have a minimal impact on the output values for simulations. The overall thrust was not affected by the addition of the N242 walls, in both Earth and Martian testing, and for both 1- and 2-Stack setups. The use of the blast shields and test stand do have some effect that must be noted, but the effect is limited when testing in Martian conditions, only around 10 percent, resulting in a thrust change of around 0.05 N for 1-Stack and 0.2 N for 2-Stack. It has a more significant impact at 1013 mbar, but as this is not the crucial part of testing, this will not need to be considered as heavily. In addition, recirculation did not occur in any full-setup simulation, even when run for 200 real seconds. This is largely due to limitations of the computer, which cannot provide enough grid refinement in order to accurately track all of the flow. Even when recirculation was created, using the shortened setup, the effect was minimal. This was due to the fact that only a very slow velocity flow reached the blades, which insignificantly affected the thrust. In the “worst-case” testing with the maximum velocity flow, the thrust dropped by around 40 percent in both cases.

Therefore, until more advanced simulations are run, it can be assumed that the rough geometries that will be used in hover experimentation in the N242 pressure chamber will not have an effect on the thrust values, if run for less than 200 seconds at a consistent 3,000 RPM. If the PAL is run for a longer duration at this speed, or with a sweep of RPMs, it is possible that recirculation could occur. However, it would take a very long time for recirculation at a large velocity to re-reach the blades and actually affect the output values.

FUTURE WORK

Future efforts should be made to generate recirculation in RotCFD. A more powerful computer or different methods of coarsening may be able to generate accurate recirculation. One potential solution would involve using a very powerful computer with the full setup and AGR, which would be able to track the flow and ensure the correct amount of refinement is occurring. Another consideration would be including some of the anomalies of N242 not placed in this model. There are platforms and other objects in the PAL that would impact flow, and they should be considered as well when dealing with flow away from the testing setup.

Efforts should also be put toward better organizing the previous data for testing. A database of previously examined testing conditions and results would be infinitely helpful to continuing research on the MH. A rough draft was created throughout this project, but an official spreadsheet would be helpful. The limitations of the computers used for future research should be considered, and extra special care should be taken in the setup, ensuring that key conditions are checked before each run. A significant amount of time was lost because setups were saved incorrectly.

REFERENCES

- Boles, Mason. *Mars Scout Helicopter Testing and Analysis*. Ball State University, Muncie, Indiana. 2016. Accessed June 2017.
- Johansson, Marcus: Experimental and Computational Evaluation of Capabilities of Predicting Aerodynamic Performance for a Mars Helicopter Rotor. MS Thesis, Department of Applied Mechanics, Chalmers University of Technology, Gothenburg, Sweden, 2017.
- Koning, W. J. F.; Johnson, W.; and Allan, B. G.: Generation of Mars Helicopter Rotor Model for Comprehensive Analyses. AHS Technical Meeting on Aeromechanics Design for Vertical Lift, San Francisco, CA, Jan. 16–18, 2018.
- McCoy, Miranda; Wadcock, Alan J.; and Young, Larry A.: Documentation of the Recirculation in a Closed-Chamber Rotor Hover Test. NASA/TM–2016-219162, Aug. 2016.

APPENDIX A: RAW DATA

1013 mbar 1-Stack

Table A1. Raw Data for 1013-mbar 1-Stack Runs

	Test 1	Test 2	Test 3	Test 4	Test 5	Test 6	Test 7	Test 8	Test 9
Setup:									
Stacks	1	1	1	1	1	1	1	1	1
Pressure (mbar)	1013	1013	1013	1013	1013	1013	1013	1013	1013
Thrust Dir.	UP	UP	UP	UP	UP	UP	UP	UP	UP
RPS	50	50	50	50	50	50	50	50	50
Unsteady	N	N	Y	N	N	N	N	N	N
Flight Condition	FSV 0	FSV 0	FSV 0	FSV 0	FSV 0	FSV 0	FSV 0	FSV 0	FSV 0
Processing	OpenMP	OpenMP	OpenMP	OpenMP	OpenMP	OpenMP	OpenCL	OpenCL	OpenCL
Grid:									
Refinement Box	5	5	5	5	5	5	5	5	5
Rotor Refinement	7	7	7	7	7	7	7	7	7
Min. Cell Size	0.0625	0.0625	0.0625	0.0625	0.0625	0.0625	0.0625	0.0625	0.0625
Adaptive	AGR	NAGR	NAGR	NAGR	NAGR	NAGR	NAGR	NAGR	NAGR
Cells	1681192	1681192	1681192	1681192	866624	866624	866624	866624	1681192
Grid Change	N	N	N	N	Y	Y	Y	Y	N
Output:									
Restart Int.	2000	2000	2000	100	2000	100	100	100	100
Completed Steps	1500	570	334	612	109	702	1100	500	7200
Total Steps	5000	7200	7200	7200	7200	5000	5000	500	7200
Completed Time	0.6	0.158333	0.0927778	0.17	0.030278	0.2808	0.44	2	2
Total Time	2	2	2	2	2	2	2	2	2
# Rotations	30	7.916667	4.6388889	8.5	1.513889	14.04	22	100	100
Results:									
CT	0.01249			0.012489		0.01249	0.0126	0.0127	0.01254
Thrust (N)	325	355	319	323.9	329	323.03	325.9	328.3	324.3
Power (W)	6211	6100	6250	6244.8	...	6246.7	6230.9	6351	6184.9
Status:	Done	Done	Done	Done	Done	Done	Done	Done	Done
Comment:	AGR	unsteady	shutdown		Grid		OpenCL	Short	Complete

1013 mbar 2-Stack

Table A2. Raw Data for 1013-mbar 2-Stack Runs

	Test 1	Test 2	Test 3	Test 4	Test 5
Setup:					
Stacks	2	2	2	2	2
Pressure (mbar)	1013	1013	1013	1013	1013
Thrust Dir.	UP	UP	UP	UP	UP
RPS	50	50	50	50	50
Unsteady	N	N/Y	N	N/Y	N
Flight Condition	FSV 0	FSV 0	FSV 0	FSV 0	FSV 0
Processing	OpenCL	OpenCL	OpenCL	OpenCL	OpenCL
Grid:					
Refinement Box	5	5	5	4	5
Rotor Refinement	7	7	7	8	7
Min. Cell Size	0.0625	0.0625	0.0625	0.0625	0.0625
Adaptive	NAGR	NAGR	NAGR	NAGR	NAGR
Cells	1737696	1737696	1737696	1015296	1737696
Grid Change	N	N	N	Y	N
Output:					
Restart Int.	100	100	100	100	100
Completed Steps	531	5700	901	3630	500
Total Steps	7200	7200	7200	7200	500
Completed Time	0.1475	1.583333	0.250278	1.008333	2
Total Time	2	2	2	2	2
# Rotations	7.375	79.16667	12.51389	50.41667	100
Results:					
CT	0.020551	0.02056	0.020756	0.020886	0.02116
Thrust (N)	532.36	531.57	536.6	539.95	547
Power (W)	12305.7	11712.3	12262.5	12111	12248.4
Status:	Done	Done	Done	Done	Done
Comment:		1Unsteady		Grid	SHORT

14 mbar 1-Stack

Table A3. Raw Data for 14-mbar 1-Stack Runs

SETUP	Test 1	Test 2	Test 3	Test 4	Test 5	Test 6	Test 7	Test 8	Test 9	Test 10	Test 11	Test 12	Test 13	Test 14
Stacks	1	1		1			1	1	1	1	1	1	1	1
Thrust	UP	UP	UP	UP	UP	UP	UP	UP	UP	UP	UP	UP	UP	UP
Bodies	ISOL	Room	Stand	Room	Stand	Stand	FULL	FULL	FULL	FULL	VEL	LL	VEL	VEL
Tunnel Position	N/A	0	N/A		N/A	N/A	0.5	0	0	0	0	0	0	0
Processing	OpenCL	OpenCL	OpenCL		OpenCL	OpenMP	OpenCL	OpenCL	OpenCL	OpenCL	OpenCL	OpenCL	OpenCL	OpenCL
Flow Point	N/A	0	N/A			N/A	0	0	0	0	0	0	0	0
Computer	M	M	M	B	M	B	M	M	P	M		M	M	M
CONDITIONS														
Pressure	14	14		14			14	14	14	14	14	14	14	14
Density	0.01612	0.01612		0			0.01612	0.01612	0.01612	0.01612	0	0.01612	0.01612	0.01612
X	13	T	T		T	T	T	T	T	T	T	T	T	T
Y	14	T	T		T	T	T	T	T	T	T	T	T	T
Z	20	T	T		T	T	T	T	T	T	T	T	T	T
Z Properties	Pressure	Pressure	Velocity		Velocity	Velocity	Velocity	Velocity	Velocity	Velocity	Velocity	Velocity	Velocity	Velocity
Rotor Pos.	2.95	2.95					2.95	2.95	2.95	2.95	3	2.95	2.95	2.95
Max Cell Size	0.5	0.5					0.5	0.5	0.5	0.5	1	0.5	0.5	0.5
Rotor Refinement	7	7					7	7	7	7	7	7	7	7
Body Refinement	N/A	4					6	6	6	6	6	6	6	6
Wall Refinement			N/A		N/A		4	4	4	4	4	4	4	4
Turbulence	Realizable	Realizable	Realizable	Realizable	Realizable	Realizable	Realizable	Realizable	Realizable	Realizable	Realizable	Realizable	Realizable	Realizable
Refinement Box	5	N/A	N/A		N/A	N/A	N/A	N/A	N/A	N/A	N/A	N/A	N/A	N/A
RB Position	ON	N/A	BELOW		N/A	N/A	N/A	N/A	N/A	N/A	N/A	N/A	N/A	N/A
# Cells	1288000	915000					1156000	1091000	1091000	1300000				
Boundary Refine	1	1					1	1	1	4		4	4	4

Table A3. Raw Data for 14-mbar 1-Stack Runs (continued)

SETUP	Test 1	Test 2	Test 3	Test 4	Test 5	Test 6	Test 7	Test 8	Test 9	Test 10	Test 11	Test 12	Test 13	Test 14
TIME														
Restart Int.	100	100					100	100	250	250		250	250	250
Completed Steps	127	3704					14381	5116	14253	20000		20000	5000	5000
Total Steps	7200	15000					20000	20000	20000	20000		20000	5000	5000
Total Time	2	15					200	200	200	200		200	200	200
Completed Time	0.035278	3.704		##			143.81	51.16	142.53	200	##	200	200	200
TS/RT Ratio	0.000278	0.001		##			0.01	0.01	0.01	0.01	##	0.01		
# Rotations	1.763889	185.2		##			7190.5	2558	7126.5	10000	##	10000		
Relaxation	0.1	0.1						0.1	0.1	0.1		0.1	0.1	0.1
OUTPUT														
Thrust	1.69	1.676					1.63	1.6	1.608	1.65	2	1.605	0.9915	0.9756
Power	67.5	74.69					74.5	74.322	74.5	74.8	74	73.6	66.373	66.08
CT	0.004969	0.004924					0.00479	0.00469	0.04724	0.00485	0	0.004717	0.002914	

14 mbar 2-Stack

Table A4. Raw Data for 14-mbar 2-Stack Runs

SETUP	Test 1	Test 2	Test 3	Test 4	Test 5	Test 6	Test 7	Test 8	Test 9
Stacks	2	2	2		2	2	2	2	3
Thrust	UP	UP	UP	UP	UP	UP	UP	UP	UP
Bodies	ISOL	ISOL	FULL	ISOL	FULL	N242	VEL	VEL	ISOL
Tunnel Position	N/A	N/A	0		0	0	0	0	0
Processing	OpenCL	OpenCL	OpenCL	OpenCL	OpenCL	OpenCL	OpenCL	OpenCL	OpenCL
Flow Point	N/A	N/A	0	0	0	0	0	0	1
Computer	M	M	P		J	J	M	M	M
CONDITIONS									
Pressure	14	14	14	14	14	14	14	14	14
Density	0	0	0	0	0.01612	0.01612	0	0.01612	0
X		13	T	T	T	T	T	T	T
Y		14	T	T	T	T	T	T	T
Z		10	T	T	T	T	T	T	T
Z Properties		Pressure	Velocity	Velocity	Velocity	Velocity	Velocity	Velocity	Velocity
Rotor Pos.		3	3	3	2.95	2.95	3	2.95	3
Max Cell Size		1	1	1	0.5	0.5	1	0.5	1
Rotor Refinement		9	7	7	7	7	7	7	7
Body Refinement		N/A	6	6	6	6	6	6	6
Wall Refinement		N/A	4	4	4	1	4	4	4
Turbulence Refinement		Realizable	Realizable	Realizable	Realizable	Realizable	Realizable	Realizable	Realizable
Box		5	N/A	N/A	N/A	5	N/A	N/A	N/A
RB Position		ON	N/A	N/A	N/A	below	N/A	N/A	N/A
# Cells		1				1129804			

APPENDIX B: PREVIOUS DATA

Table B1. 1013-mbar 1-Stack AGR Sweep Data (Koning)

AWT Thrust RotCFD AGR					
Single Prop, Isolated Hover, AGR, Trusting Up, 1013 mbar (Koning)					
RPM [-]	CT [-]	T [N]	P [W]	RPM ² [-]	RPM ³ [-]
500	0.009492	6.82293	24.7342	250000	125000000
1000				1000000	1000000000
1500	0.011386	73.6625	672.365	2250000	3375000000
2000	0.011641	133.883	1602.68	4000000	8000000000
2500	0.011855	213.043	3180.11	6250000	15625000000

Table B2. 1013-mbar 1-Stack NAGR Sweep Data (Koning)

AWT Thrust RotCFD NAGR					
Single Prop, Isolated Hover, Trusting Up, 1013 mbar (Koning)					
RPM [-]	CT [-]	T [N]	P [W]	RPM ² [-]	RPM ³ [-]
500	0.010746	7.72432	26.7135	250000	125000000
1000	0.012465	35.8408	210.068	1000000	1000000000
1500	0.013092	84.6966	715.969	2250000	3375000000
2000	0.01344	154.576		4000000	8000000000
2500				6250000	15625000000

Table B3. 1013-mbar 1-Stack Experimental Sweep Data (Boles)

RTF Run 5 2-bladed 40x22 thrusting up				
AWT Thrust (Mason Boles, Fig. 69)				
RPM [-]	CT [-]	T [lb]	T [N]	RPM ² [-]
525.7004		1.993791	8.868819	276360.9
1231.388		12.14251	54.01255	1516316
1724.759		23.90999	106.3569	2974793
2025.215		33.32417	148.2332	4101497

Table B4. 1013-mbar 2-Stack Casing Sweep Data (McCoy)

AWT Thrust (Miranda McCoy, Fig. 17, Green)				
2-Stacked Configuration, digitized data, 1013 mbar, with casing				
RPM [-]	CT [-]	T[lb]	T [N]	RPM^2 [-]
120.385		-0.4129	-1.83669	14492.55
502.5175		2.904263	12.9188	252523.8
1001.368		12.85718	57.19158	1002737
1497.794		30.13413	134.0432	2243386
1999.091		52.66858	234.2814	3996366
2495.032		83.90473	373.2267	6225185

Table B5. 1013-mbar 2-Stack No Casing Sweep Data (McCoy)

AWT Thrust (Miranda McCoy, Fig. 17, Blue)				
2-Stacked Configuration, digitized data, 1013 mbar, with casing				
RPM [-]	CT [-]	T[lb]	T [N]	RPM^2 [-]
254.8931		0.416033	1.850604	64970.47
502.5026		3.042087	13.53187	252508.9
1195.118		18.8004	83.62833	1428307
1497.669		33.57973	149.37	2243013
1746.699		44.08622	196.1052	3050958
1997.172		56.80302	252.6723	3988695
2247.011		71.17854	316.6178	5049060
2494.966		86.93686	386.7143	6224857

Table B6. 1013-mbar 2-Stack Experimental Sweep Data (Boles)

RTF Run 1 4-bladed 40x22 thrusting up				
AWT Thrust (Mason Boles) - redid zeros on astromed				
RPM [-]	CT [-]	T[lb]	T [N]	RPM^2 [-]
528.1552		3.147271	13.99975	278947.9
1226.846		18.98233	84.43757	1505152
1724.571		39.51513	175.772	2974144
2026.453		54.43004	242.1168	4106512

Table B7. 1013-mbar 2-Stack Simulation Data (Koning)

AWT Thrust RotCFD AGR					
2-Stacked Configuration, 1013 mbar, cumulative performance					
RPM [-]	CT [-]	T [N]	P [W]	RPM^2 [-]	RPM^3 [-]
3000	0.020942	541.919	11757.43	9000000	2.7E+10
AWT Thrust RotCFD NAGR					
2-Stacked Configuration, 1013 mbar, cumulative performance					
RPM [-]	CT [-]	T [N]	P [W]	RPM^2 [-]	RPM^3 [-]
3000	0.021699	561.506	11607.72	9000000	2.7E+10
AWT Thrust HR RotCFD NAGR Blast shield + stand					
2-Stacked Configuration, 1013 mbar, cumulative performance					
RPM [-]	CT [-]	T [N]	P [W]	RPM^2 [-]	RPM^3 [-]
3000	0.019648	507.9511	10413.04	9000000	2.7E+10
AWT Thrust HR RotCFD NAGR NO GEOM					
2-Stacked Configuration, 1013 mbar, cumulative performance					
RPM [-]	CT [-]	T [N]	P [W]	RPM^2 [-]	RPM^3 [-]
3000	0.020154	521.0446	9857.613	9000000	2.7E+10

Table B8. 1013-mbar 2-Stack Simulation Sweep (Johansson)

Hover Simulation (Johansson)		
2-Stack Configuration, 1013 mbar		
RPM	T (N)	RPM^2
1868	194.7	3489424
2100	247.3	4410000
2500	355.8	6250000
2800	452.7	7840000
3000	518.8	9000000

APPENDIX C: ROTCFD RESULTS

1013 mbar 1-Stack

Test 1:

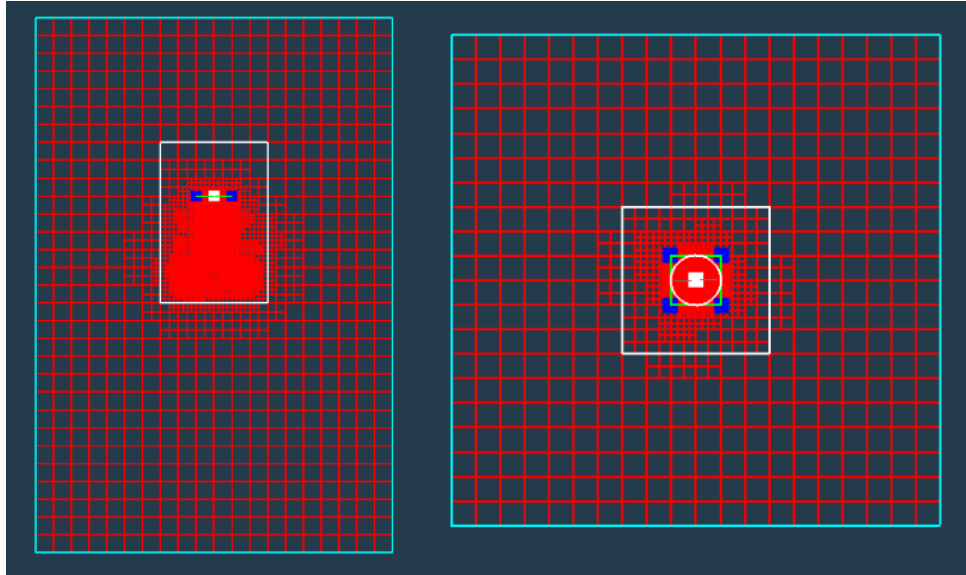


Figure C1. 1013-mbar 1-Stack test 1 isol AGR gridding.

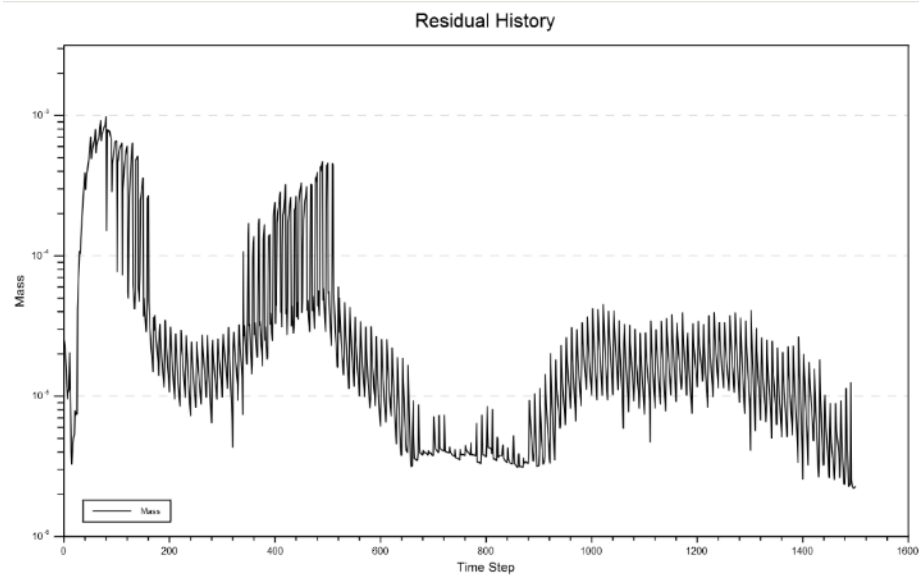


Figure C2. 1013-mbar 1-Stack test 1 isol residuals graph.

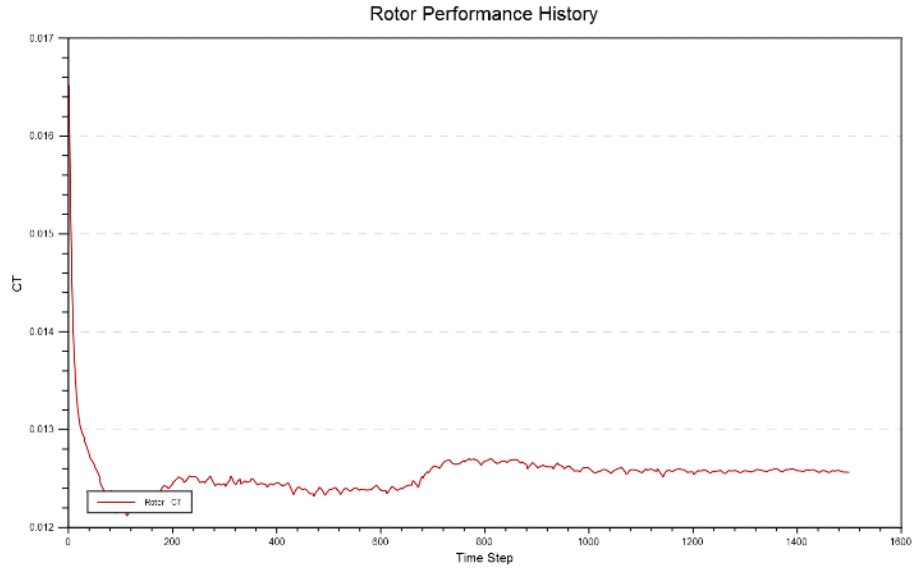


Figure C3. 1013-mbar 1-Stack test 1 isol CT graph.

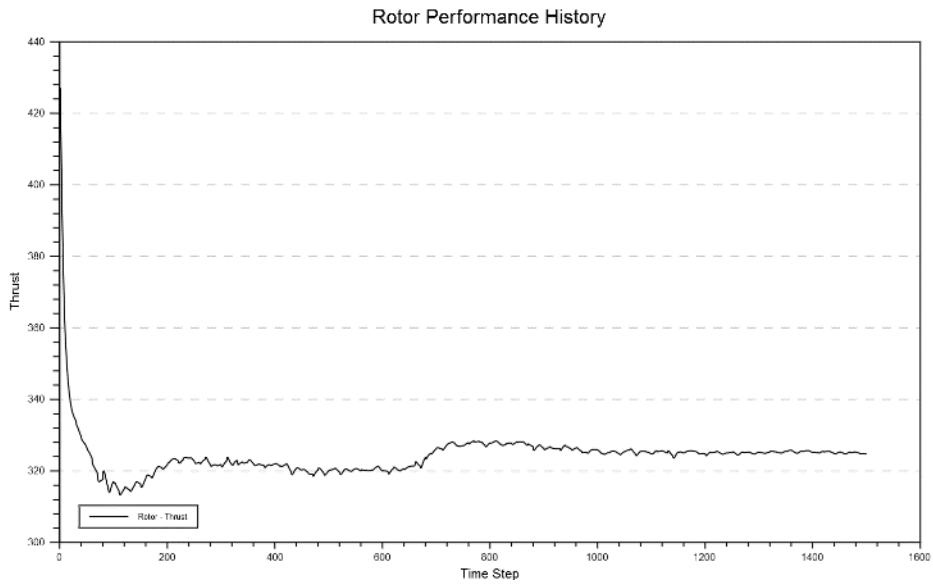


Figure C4. 1013-mbar 1-Stack test 1 isol thrust graph.

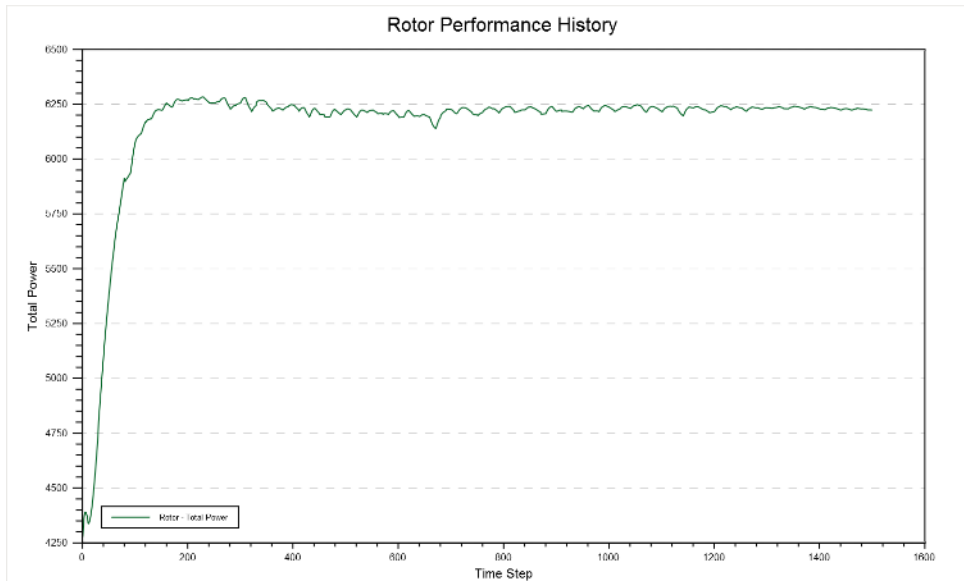


Figure C5. 1013-mbar 1-Stack test 1 isol total power graph.

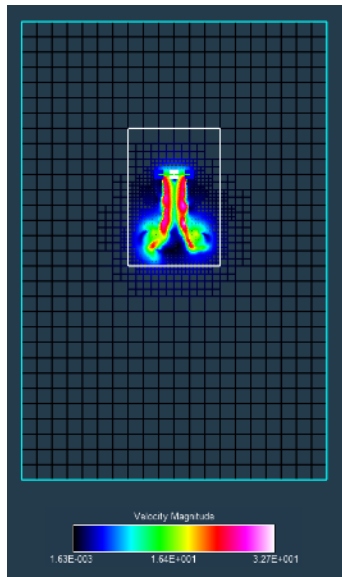


Figure C6. 1013-mbar 1-Stack test 1 isol velocity visualization.

Test 2: used unsteady condition and did not fit with any results.

Test 3: prematurely shut down because of updates; results too limited to use.

Test 4:

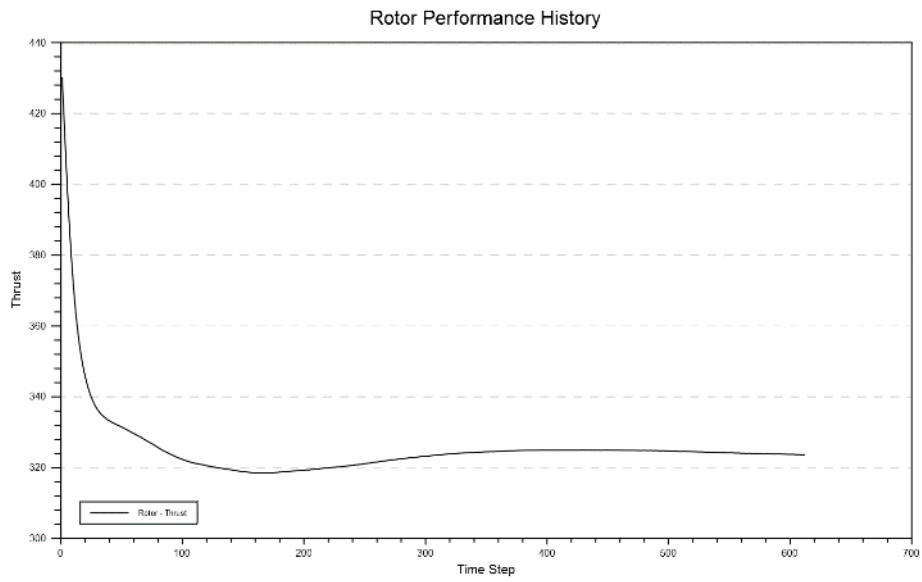


Figure C7. 1013-mbar 1-Stack test 2 isol thrust.

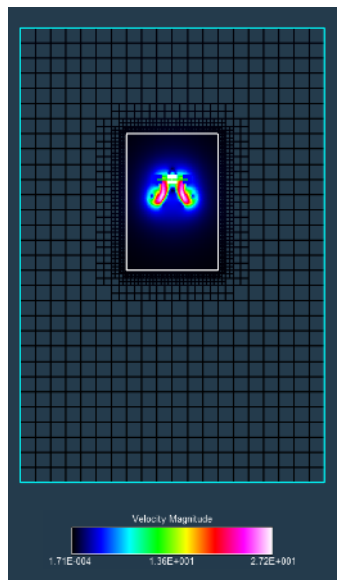


Figure C8. 1013-mbar 1-Stack test 2 isol velocity.

Test 5: stopped too early; data not converged enough to use.

Test 6:

Rotor Performance History

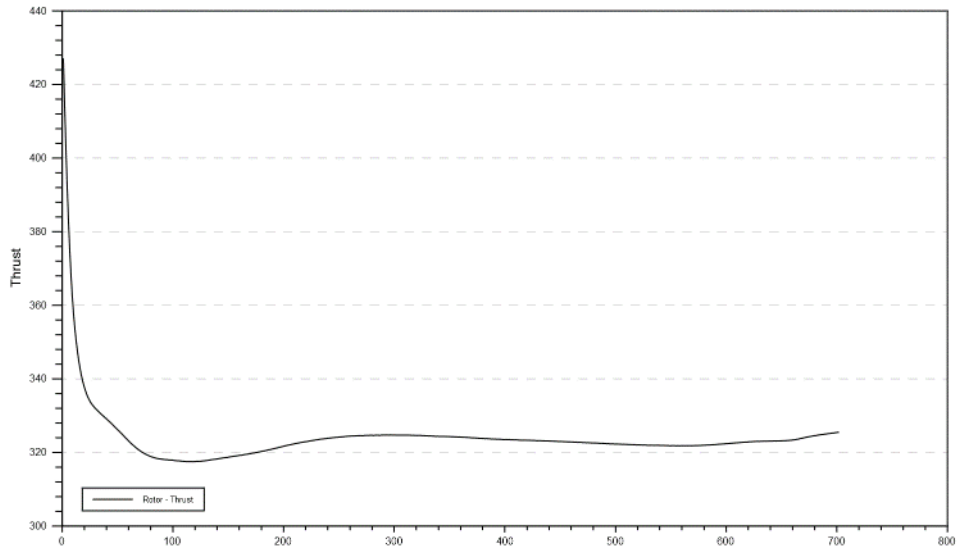


Figure C9. 1013-mbar 1-Stack test 6 isol thrust.

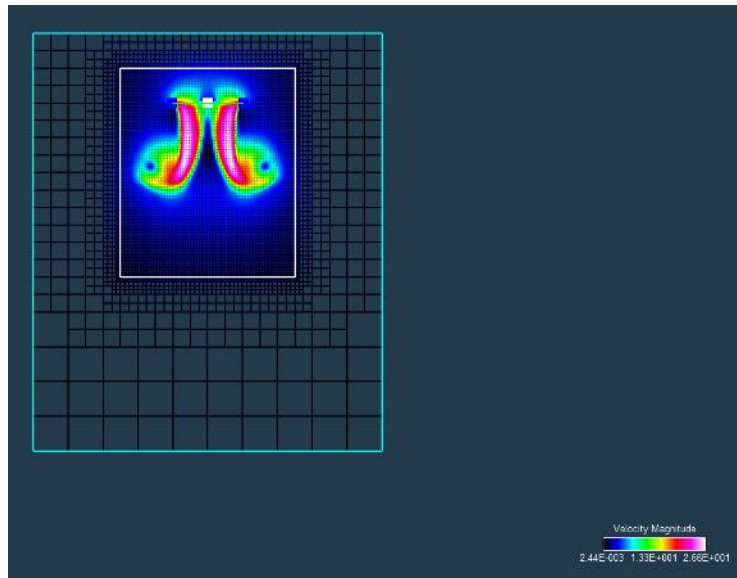


Figure C10. 1013-mbar 1-Stack test 6 isol velocity.

Test 7:

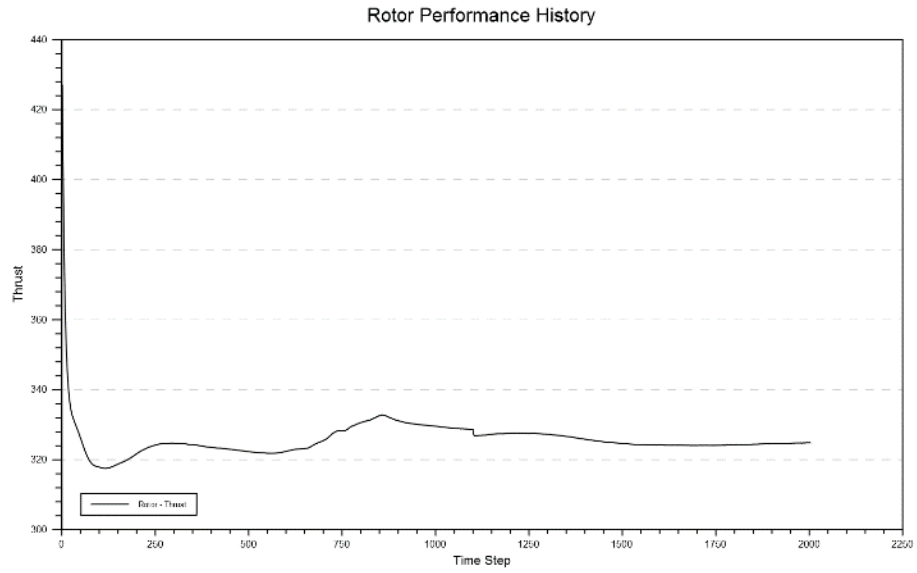


Figure C11. 1013-mbar 1-Stack test 7 isol thrust.

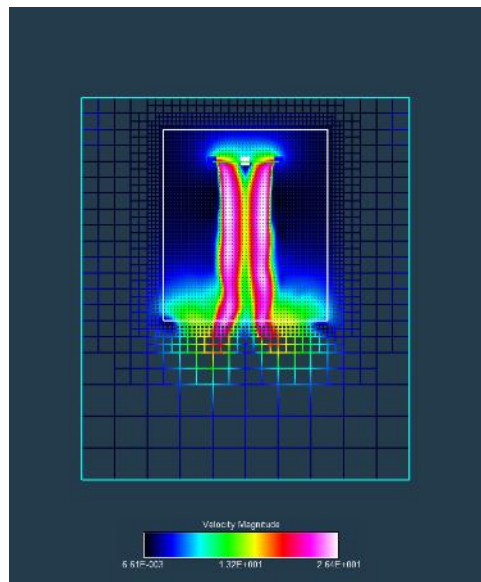


Figure C12. 1013-mbar 1-Stack test 7 isol velocity.

Test 8:

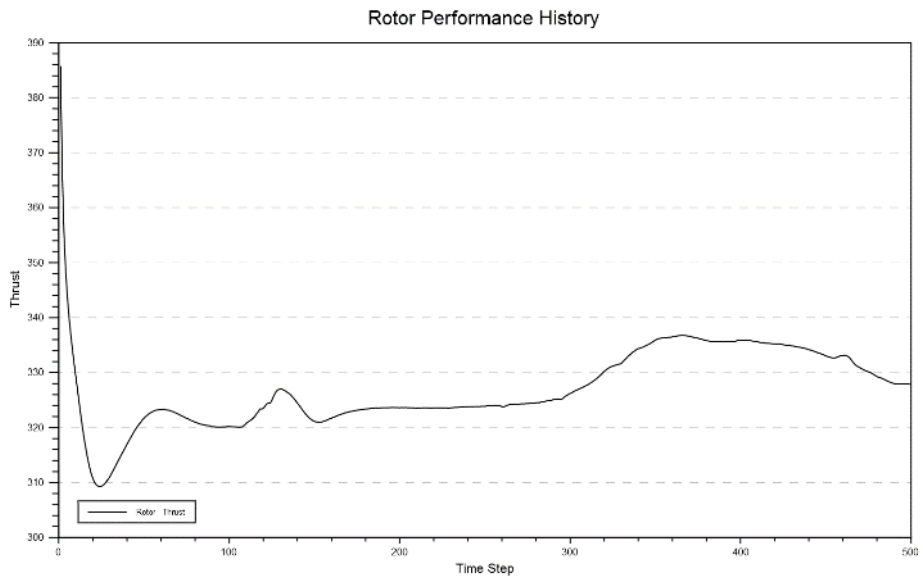


Figure C13. 1013-mbar 1-Stack test 8 isol thrust.

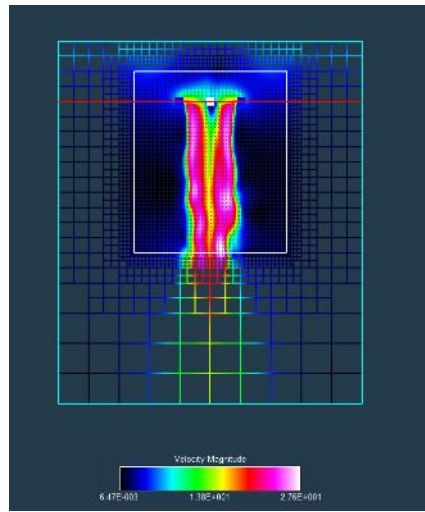


Figure C14. 1013-mbar 1-Stack test 8 isol velocity.

Test 9:

Rotor Performance History

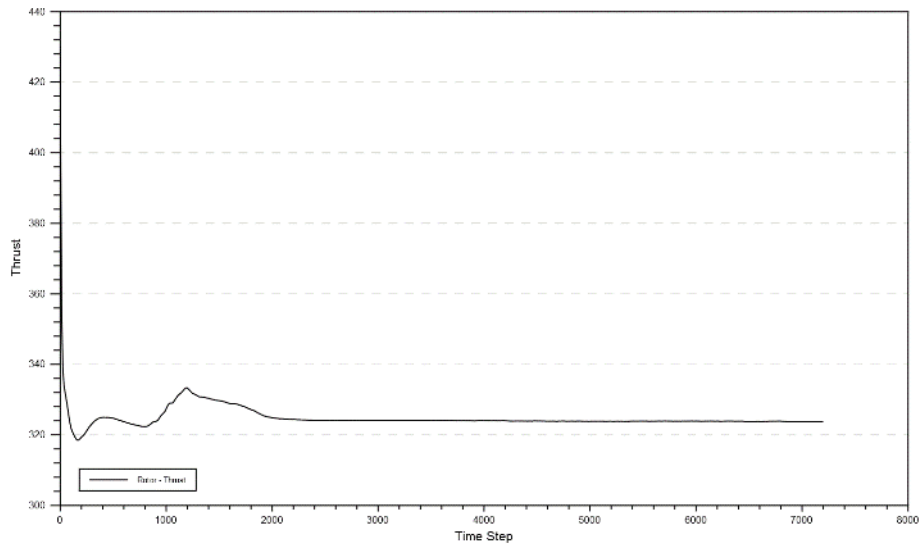


Figure C15. 1013-mbar 1-Stack test 9 isol thrust.

Test 10:

Rotor Performance History

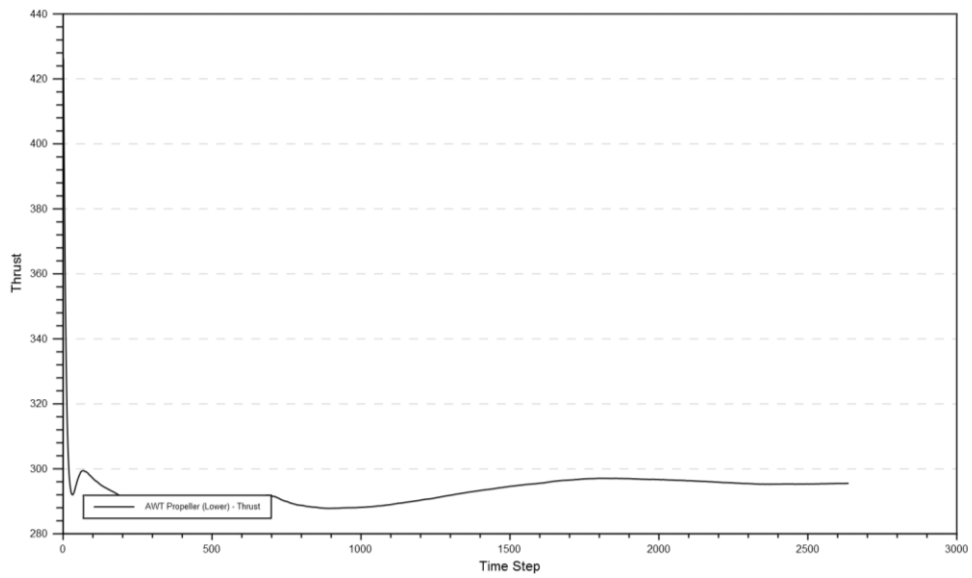


Figure C16. 1013-mbar 1-Stack test 10 full thrust.

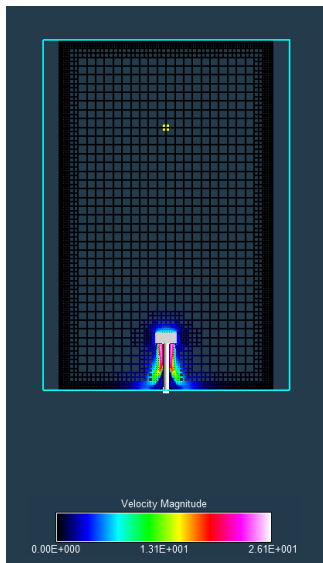


Figure C17. 1013-mbar 1-Stack test 10 velocity.

1013 mbar 2-Stack

Test 1:

Residual History

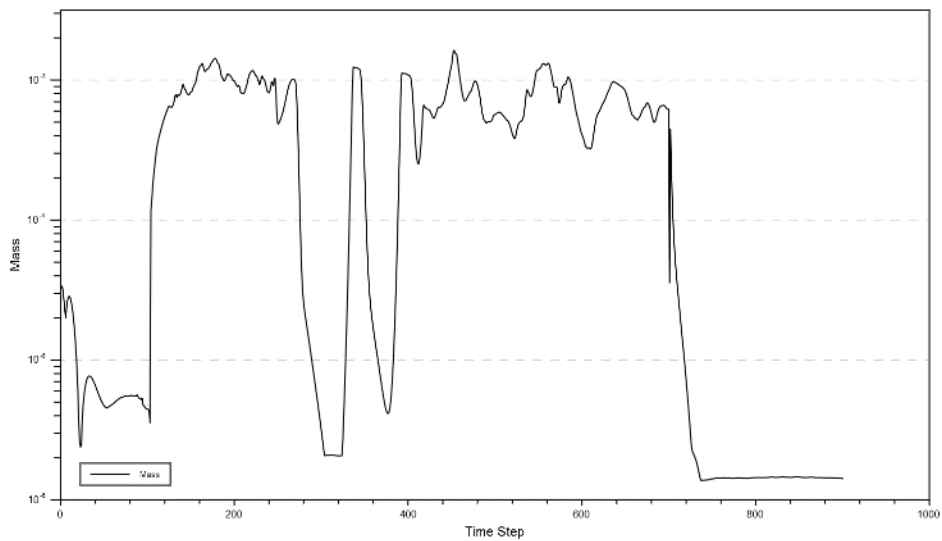


Figure C18. 1013-mbar 2-Stack test 1 isol residual.

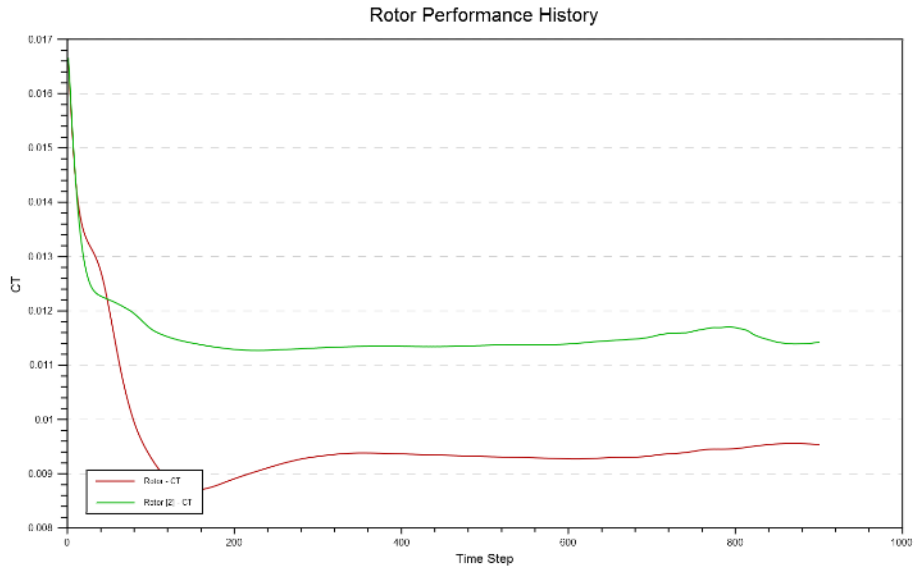


Figure C19. 1013-mbar 2-Stack test 1 isol CT.

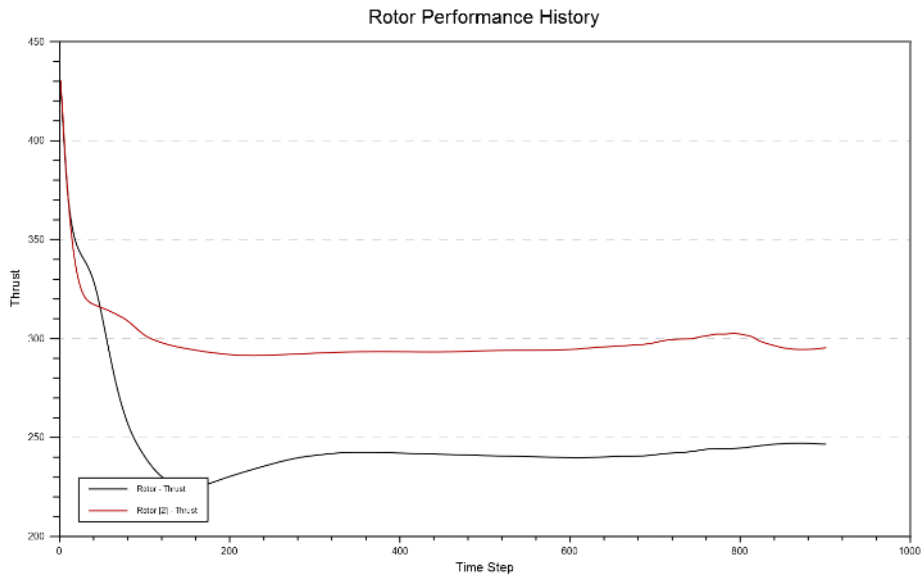


Figure C20. 1013-mbar 2-Stack test 1 isol thrust.

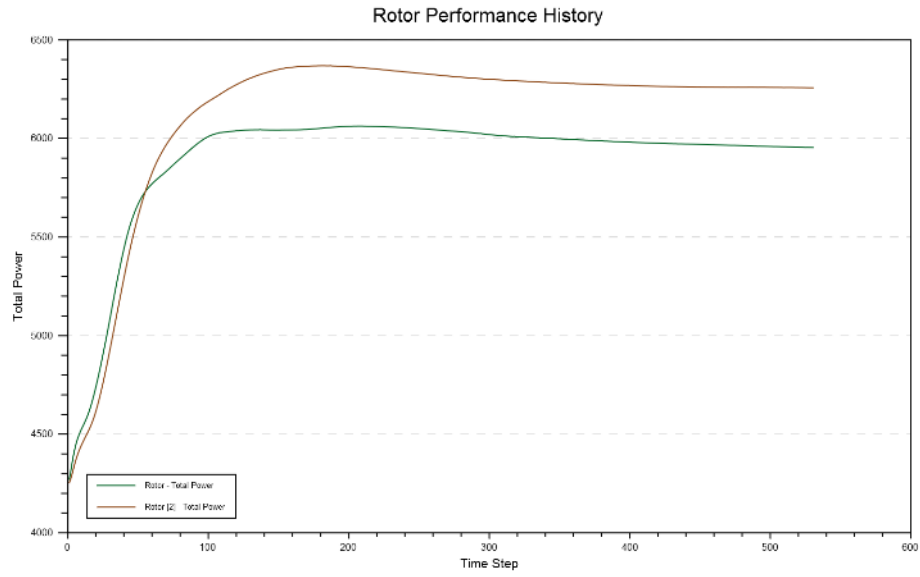


Figure C21. 1013-mbar 2-Stack test 1 isol total power.

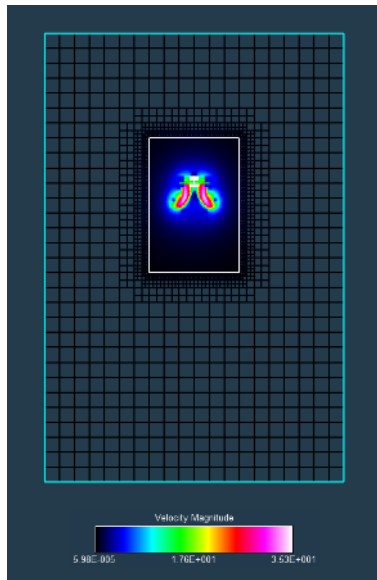


Figure C22. 1013-mbar 2-Stack test 1 isol velocity.

Test 2:

Rotor Performance History

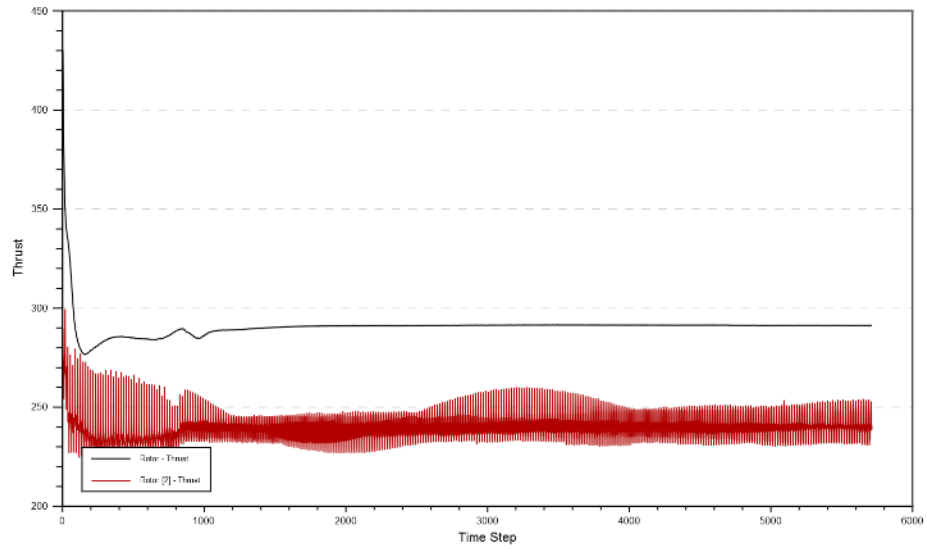


Figure C23. 1013-mbar 2-Stack test 2 isol thrust.

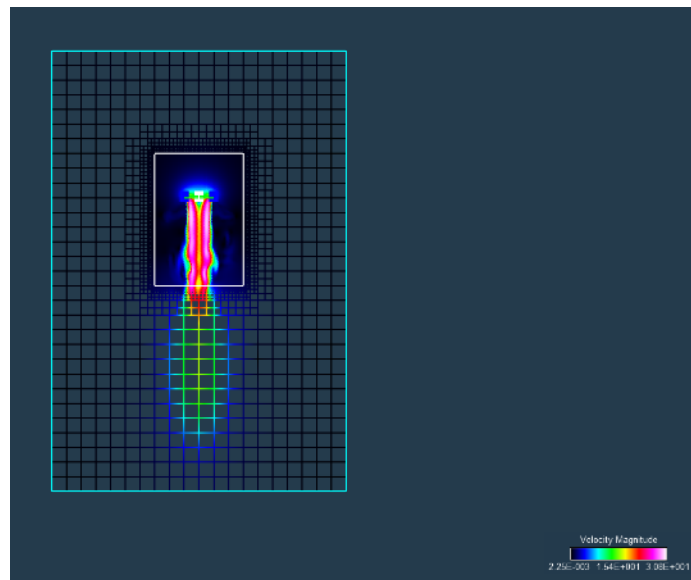


Figure C24. 1013-mbar 2-Stack test 2 isol velocity.

Test 3:

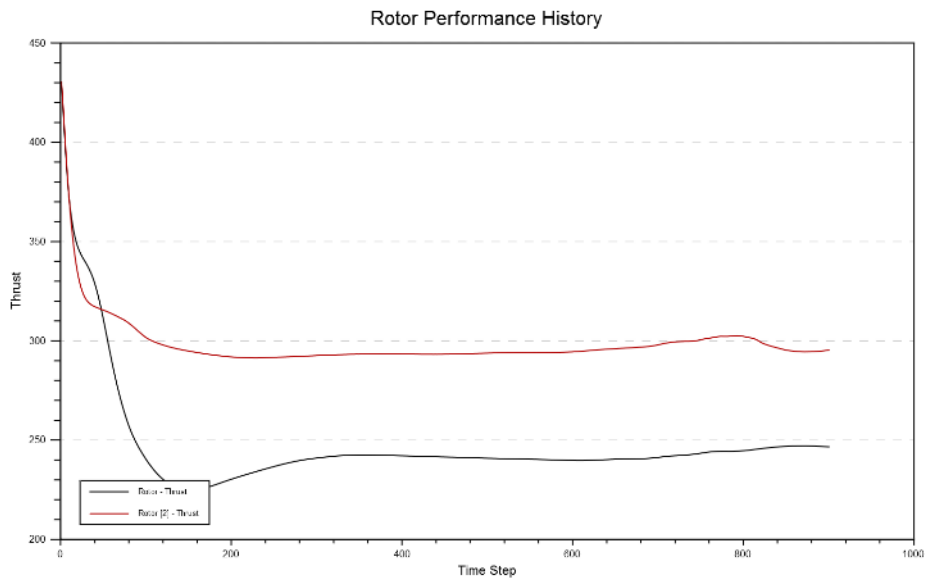


Figure C25. 1013-mbar 2-Stack test 3 isol thrust.

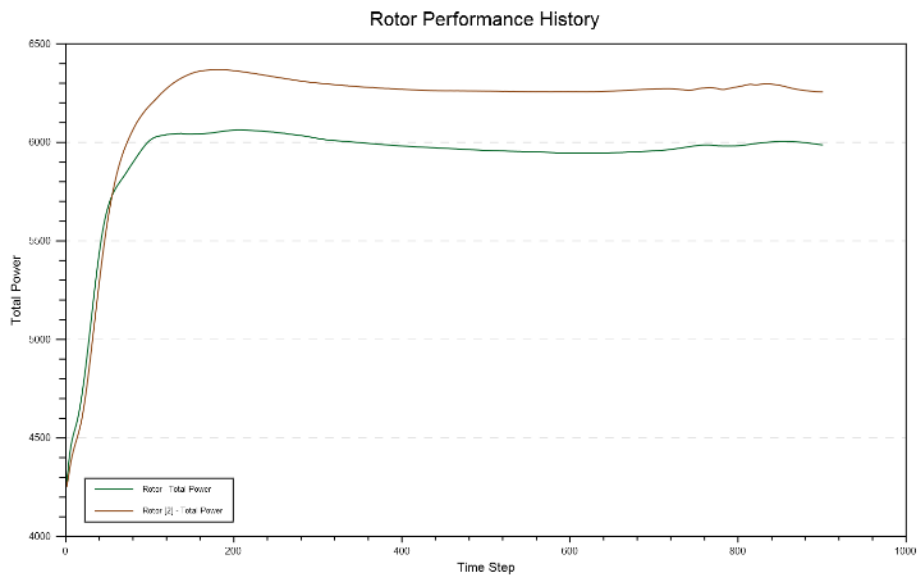


Figure C26. 1013-mbar 2-Stack test 3 isol thrust.

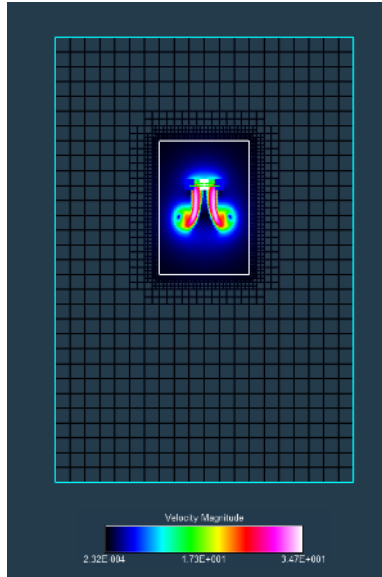


Figure C27. 1013-mbar 2-Stack test 3 isol velocity.

Test 4:

Rotor Performance History

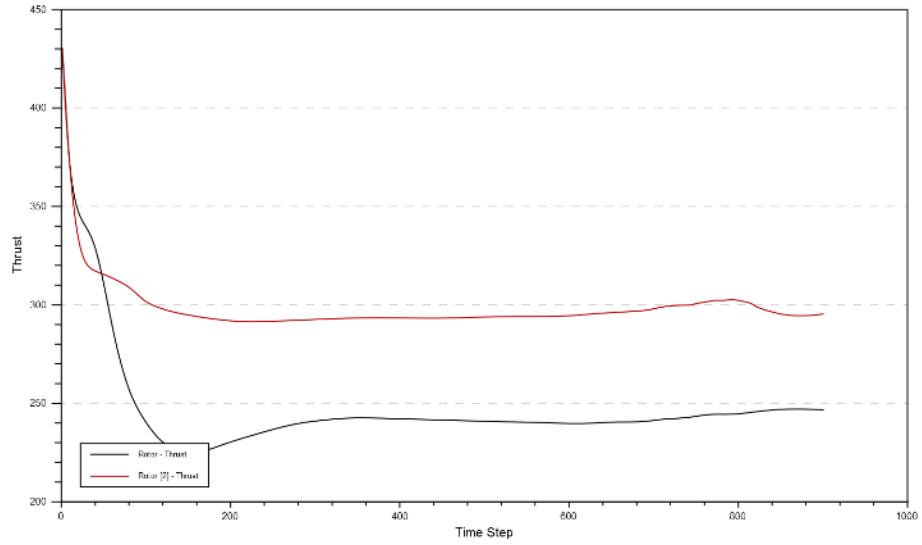


Figure C28. 1013-mbar 2-Stack test 4 isol thrust.

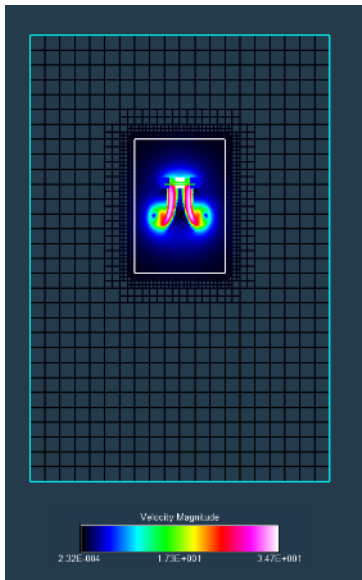


Figure C29. 1013-mbar 2-Stack test 4 isol velocity.

Test 5:

Rotor Performance History

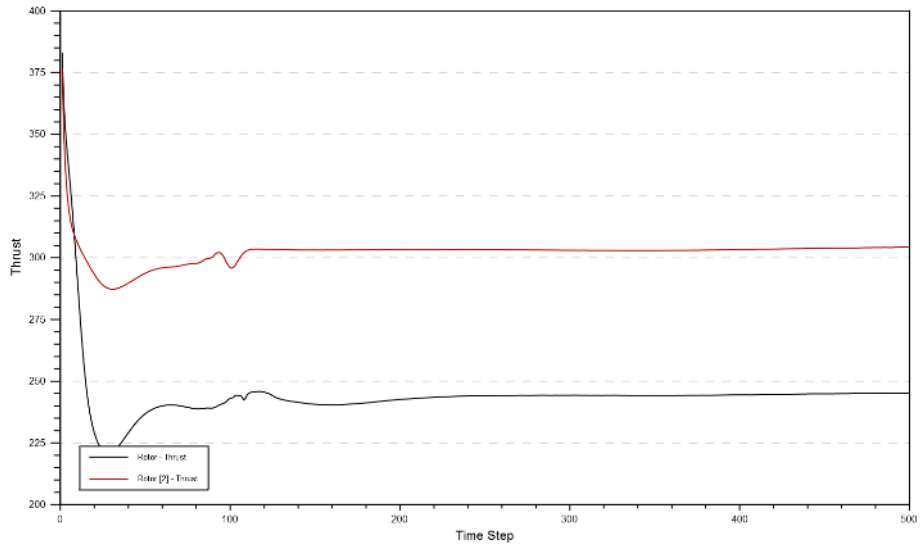


Figure C30. 1013-mbar 2-Stack test 5 isol thrust.

Test 6:

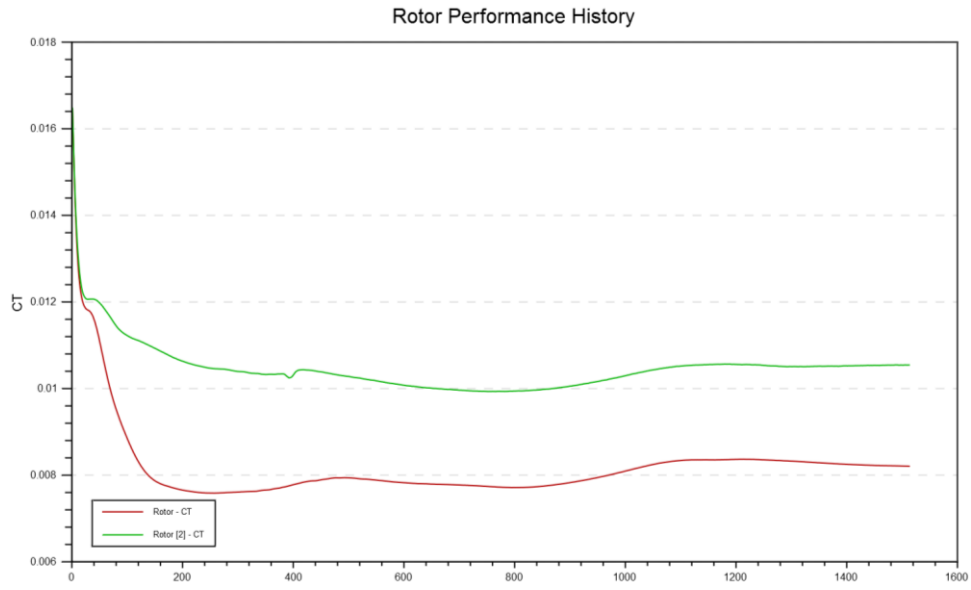


Figure C31. 1013-mbar 2-Stack test 6 isol thrust.

14 mbar 1-Stack

Test 1:

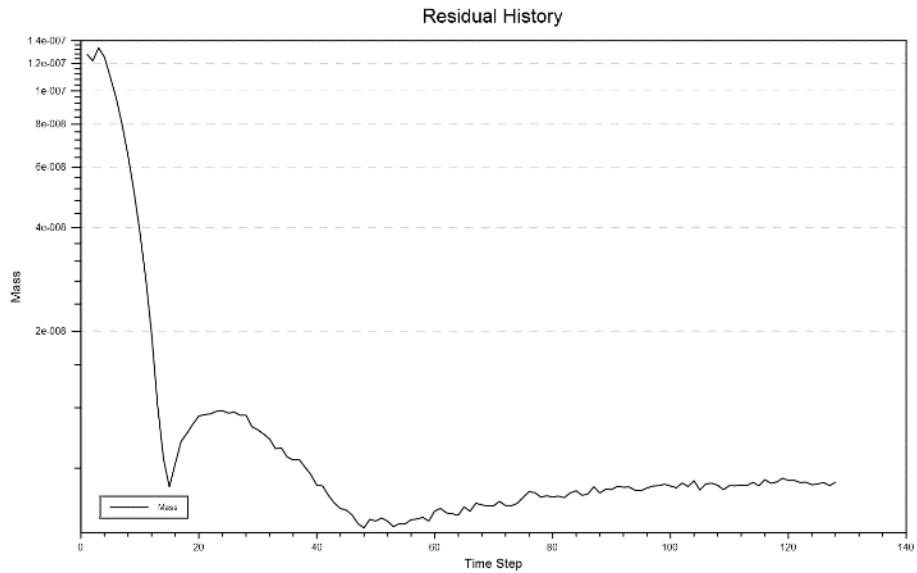


Figure C32. 14-mbar 1-Stack test 1 isol residual.

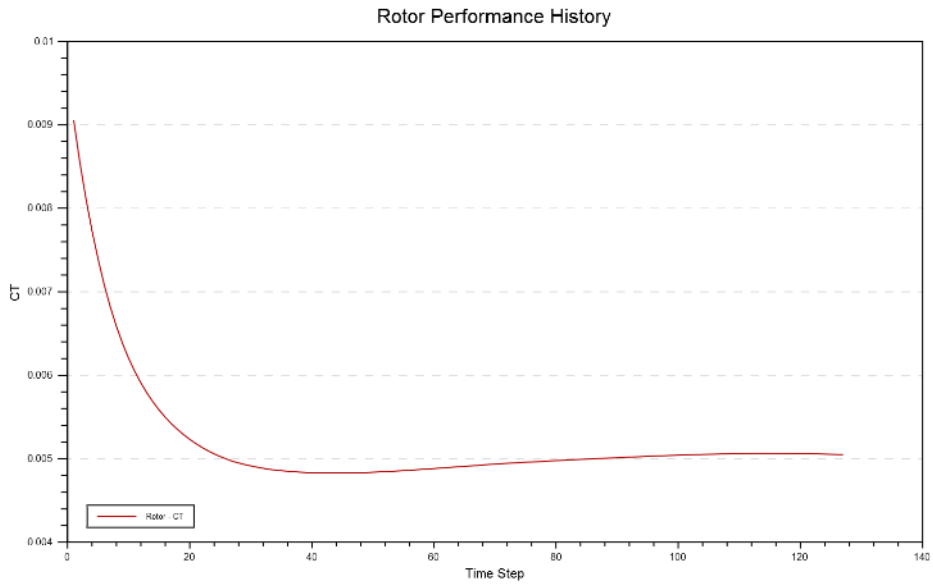


Figure C33. 14-mbar 1-Stack test 1 isol CT.

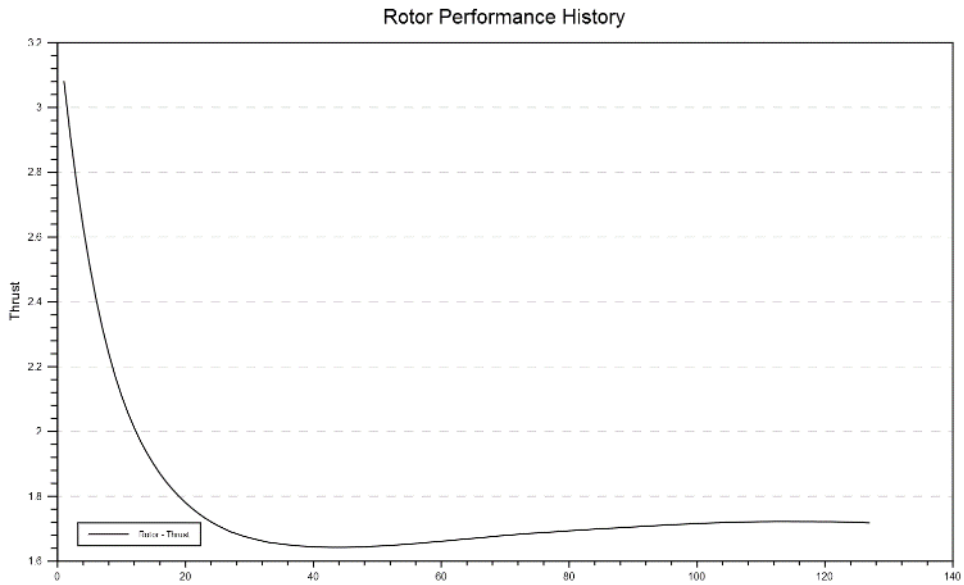


Figure C34. 14-mbar 1-Stack test 1 isol thrust.

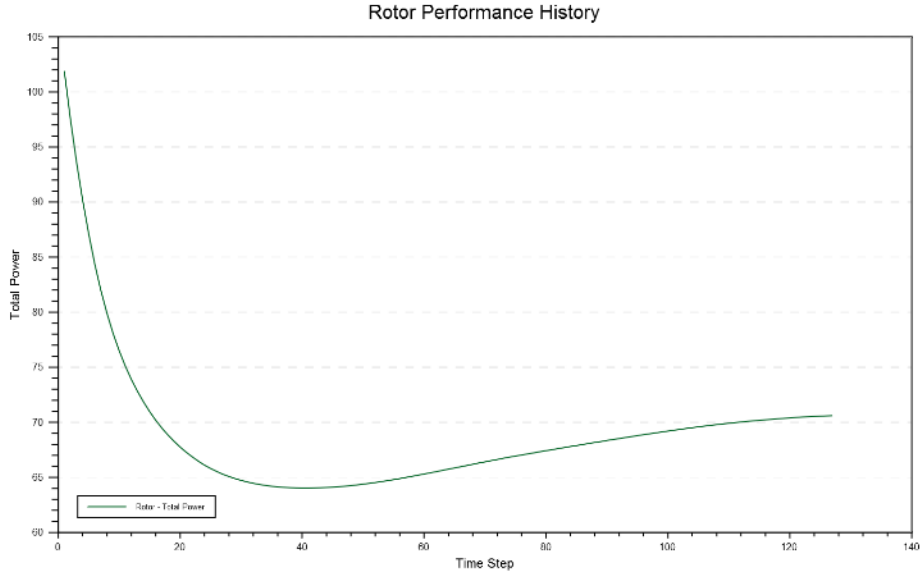


Figure C35. 14-mbar 1-Stack test 1 isol total power.

Test 2:

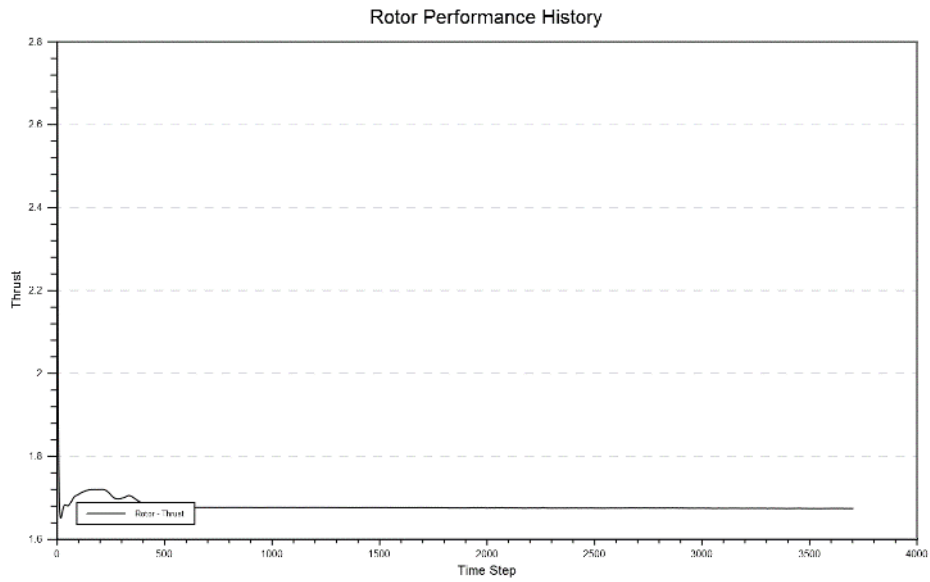


Figure C36. 14-mbar 1-Stack test 2 N242 thrust.

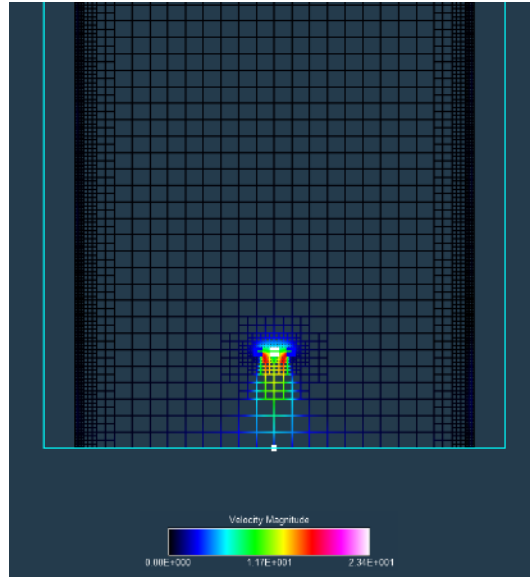


Figure C37. 14-mbar 1-Stack test 2 N242 velocity.

Test 3: flow diverged.

Test 4: lower powered computer used; bad results that diverged generated.

Test 5: flow diverged.

Test 6: flow diverged.

Test 7:

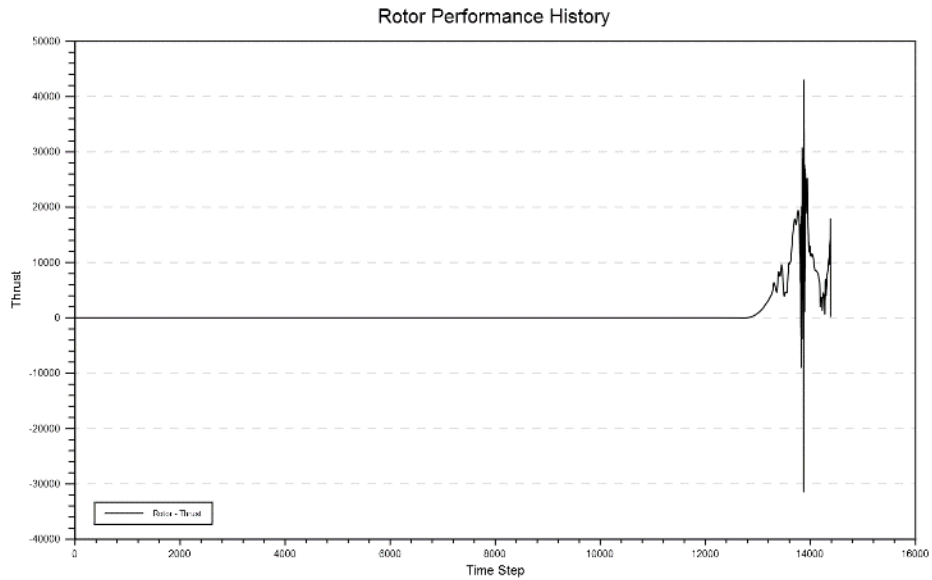


Figure C38. 14-mbar 1-Stack test 7 full thrust.

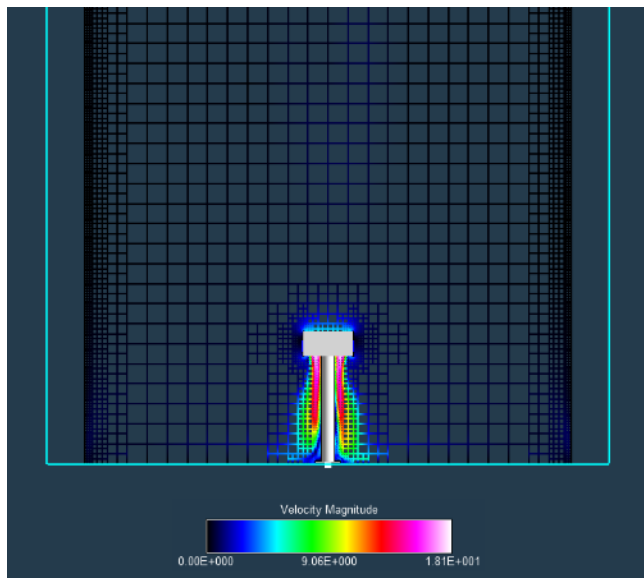


Figure C39. 14-mbar 1-Stack test 7 full velocity.

Test 8:

Rotor Performance History

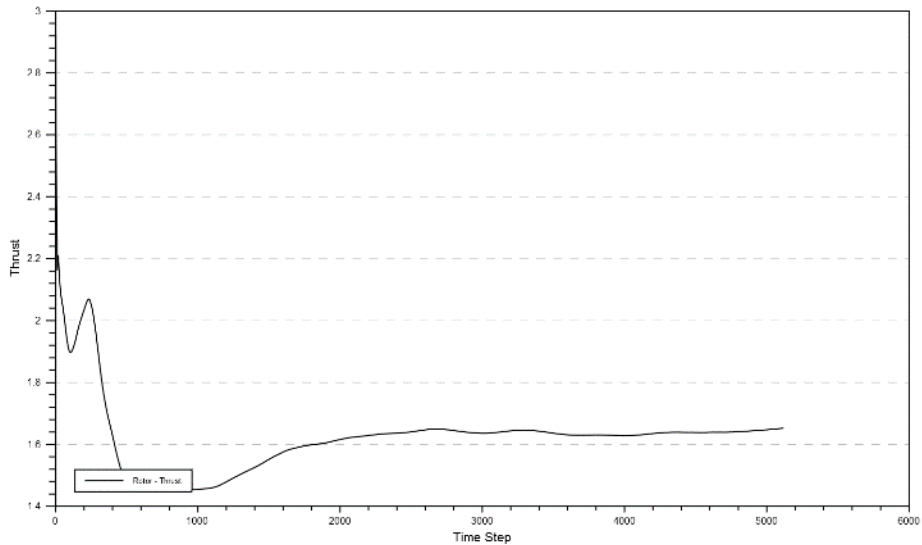


Figure C40. 14-mbar 1-Stack test 8 full thrust.

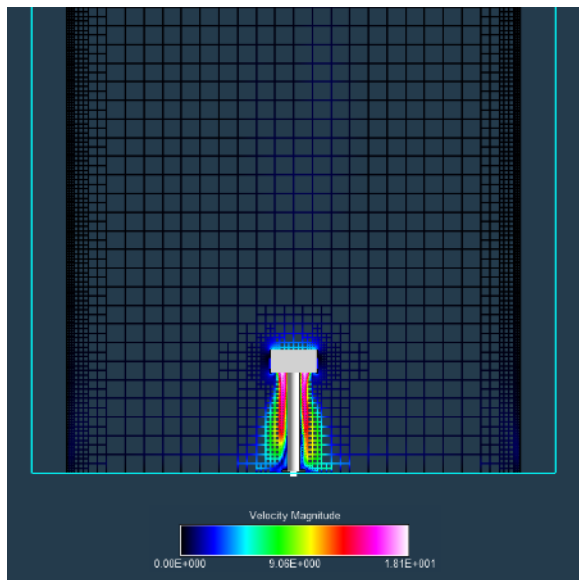


Figure C41. 14-mbar 1-Stack test 8 full velocity.

Test 9:

Rotor Performance History

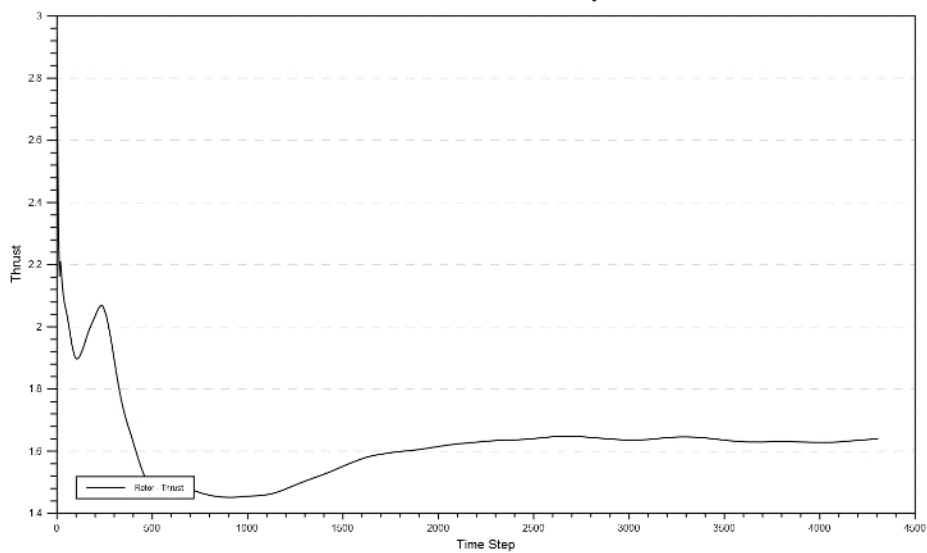


Figure C42. 14-mbar 1-Stack test 9 full thrust.

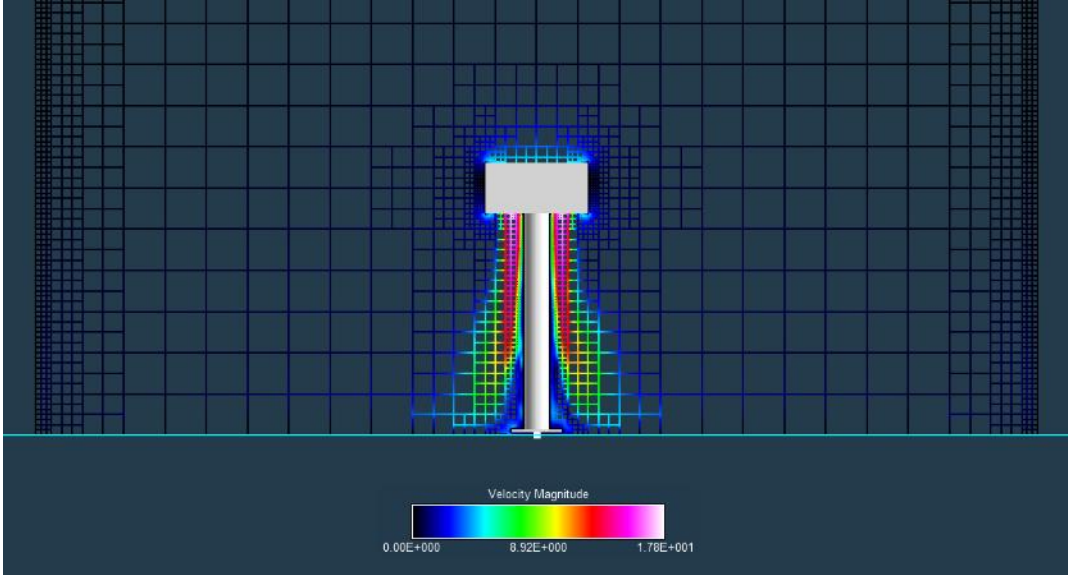


Figure C43. 14-mbar 1-Stack test 9 full velocity.

Test 10:

Rotor Performance History

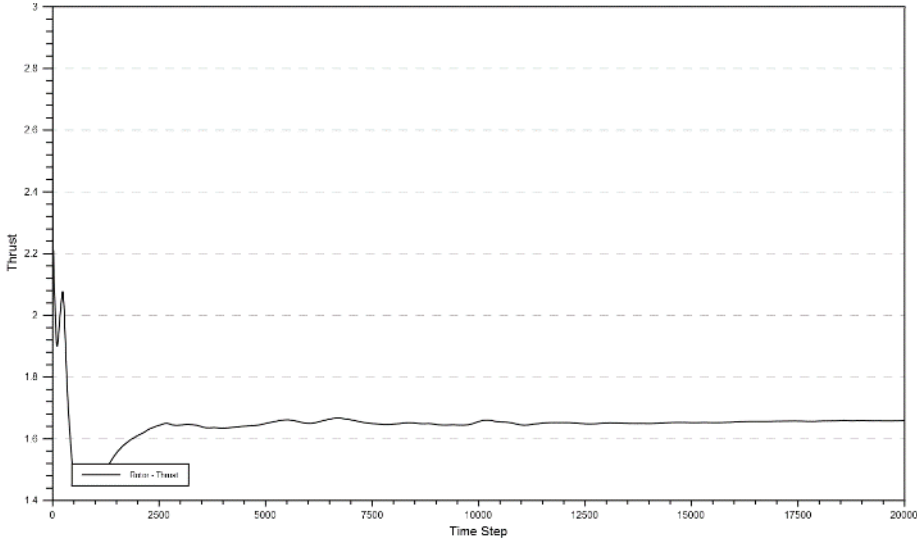


Figure C44. 14-mbar 1-Stack test 10 full thrust.

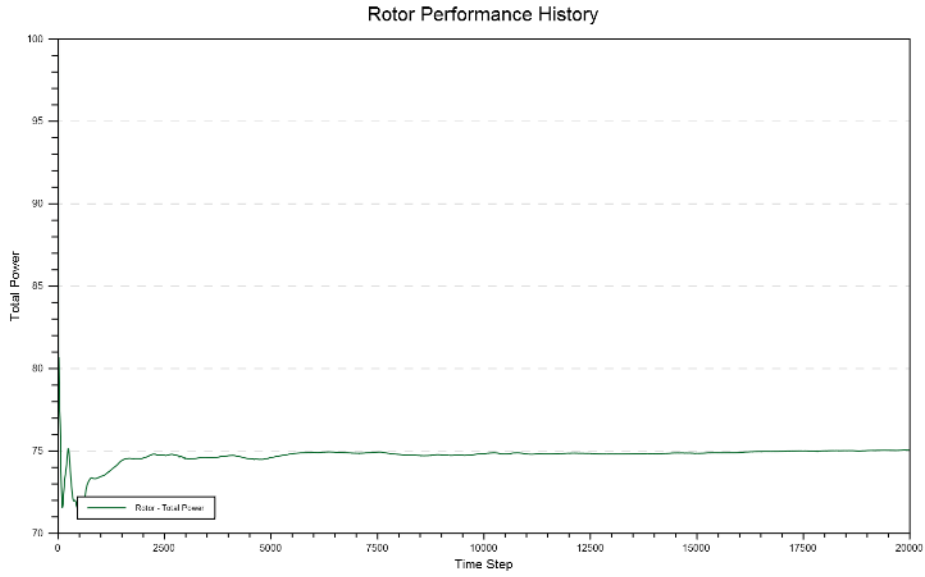


Figure C45. 14-mbar 1-Stack test 10 full total power.

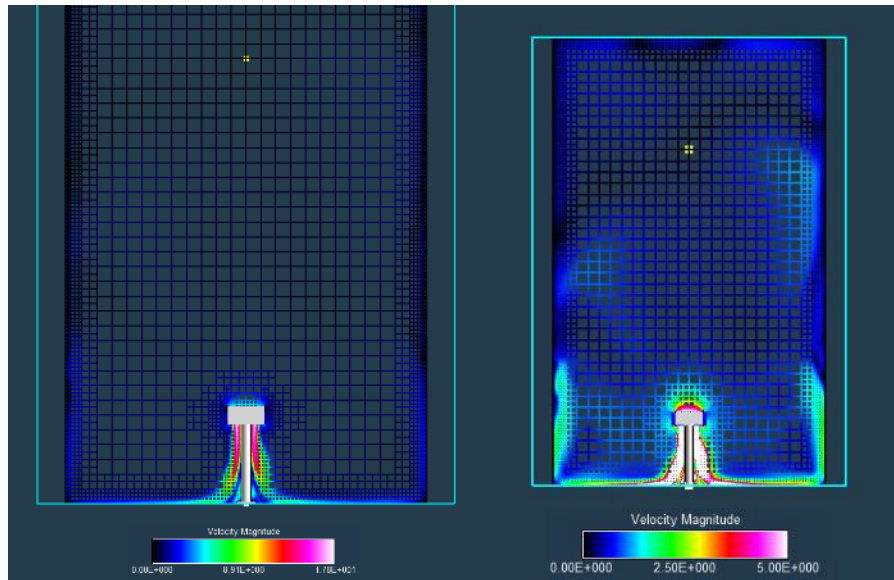


Figure C46. 14-mbar 1-Stack test 10 full velocities.

Test 11: velocity wall configurations set up incorrectly, data generated did not align.

Test 12:

Rotor Performance History

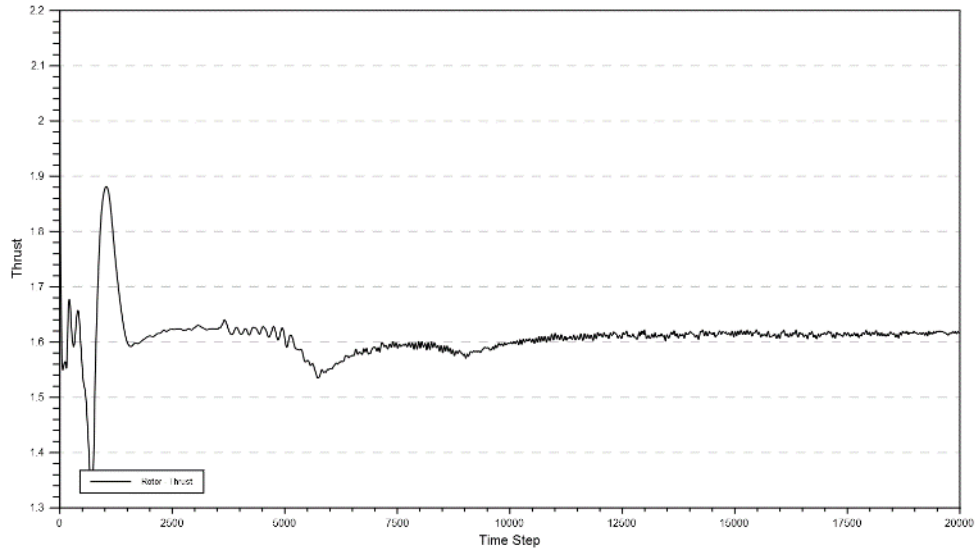


Figure C47. 14-mbar 1-Stack test 12 Laser Lab thrust.

Rotor Performance History

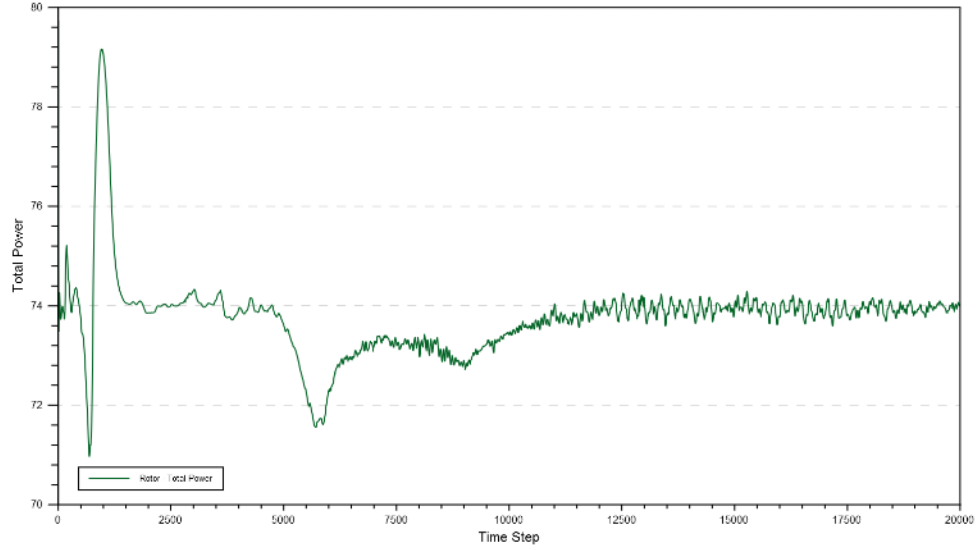


Figure C48. 14-mbar 1-Stack test 12 Laser Lab total power.

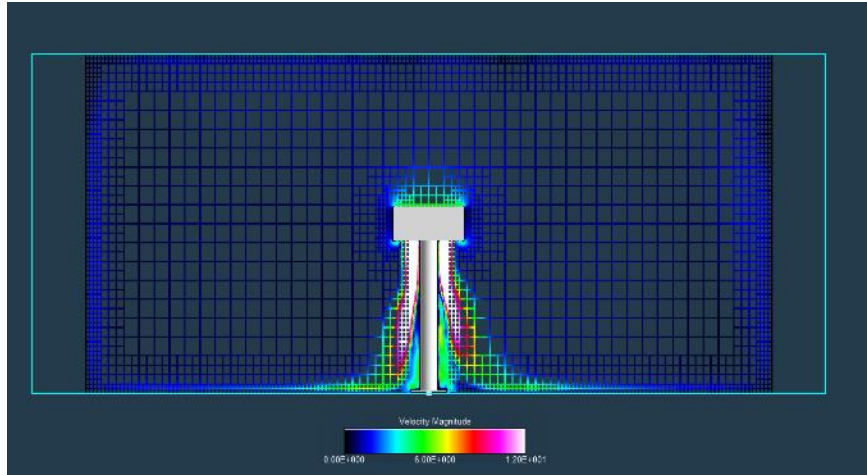


Figure C49. 14-mbar 1-Stack test 12 Laser Lab velocity.

Test 13:

Rotor Performance History

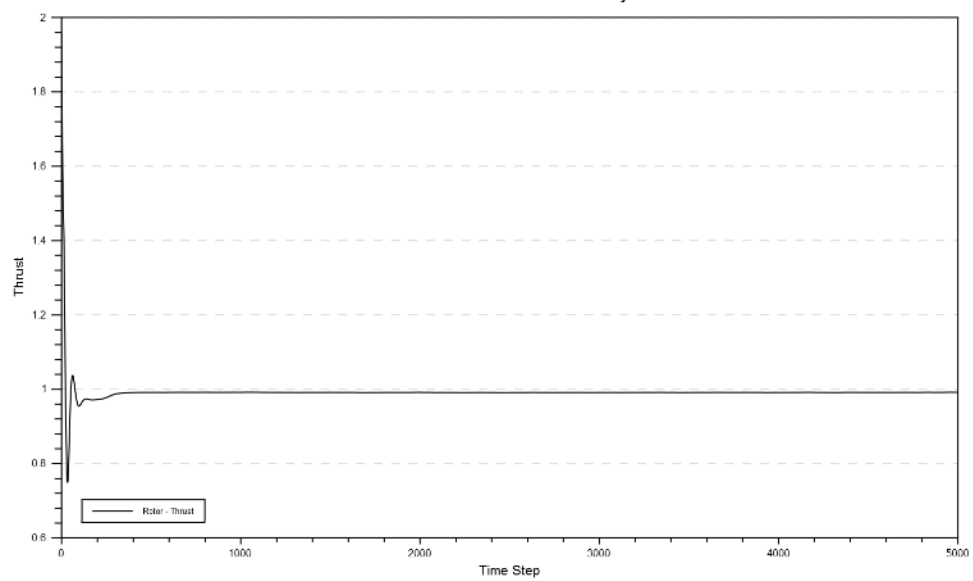


Figure C50. 14-mbar 1-Stack test 13 max velocity thrust.

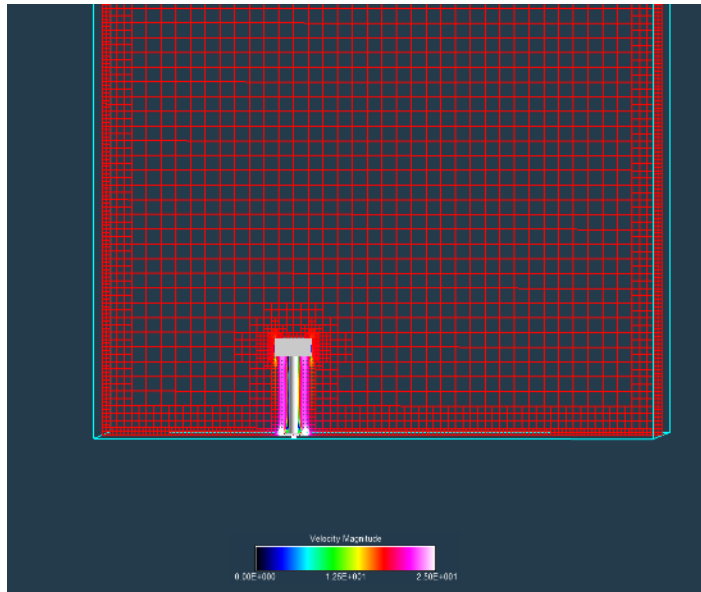


Figure C51. 14-mbar 1-Stack test 13 max velocity visualization.

Test 14:

Rotor Performance History

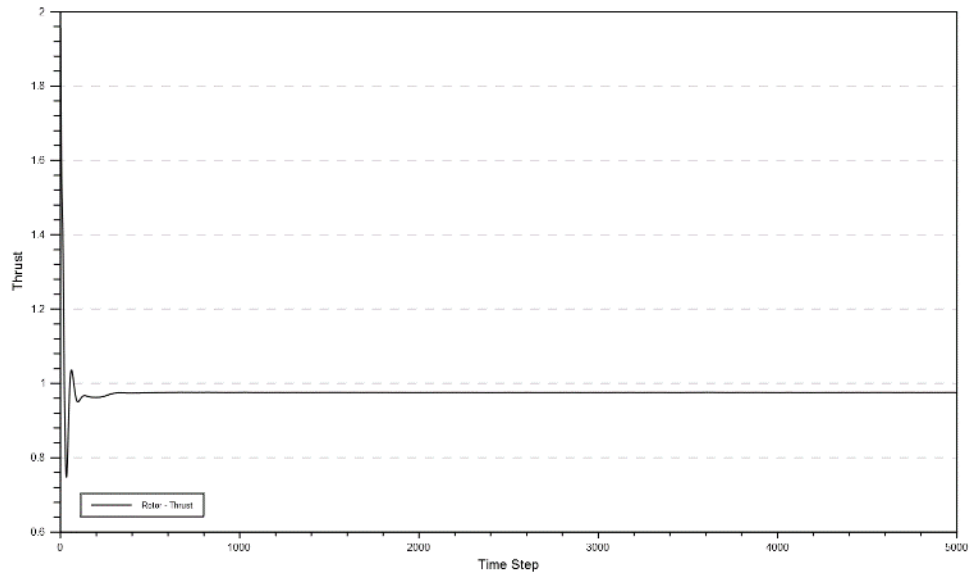


Figure C52. 14-mbar 1-Stack test 14 max velocity thrust.

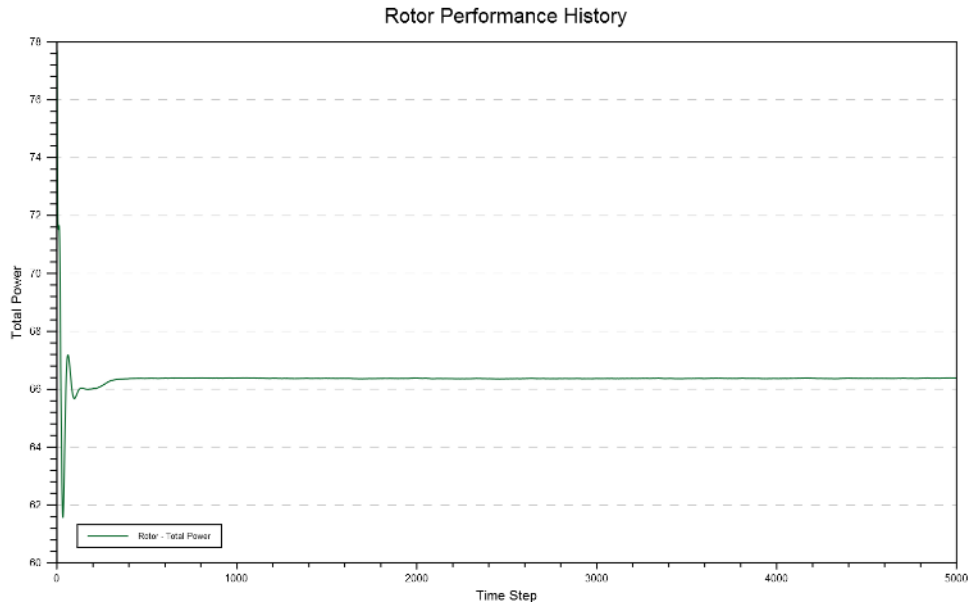


Figure C53. 14-mbar 1-Stack test 14 max velocity total power.

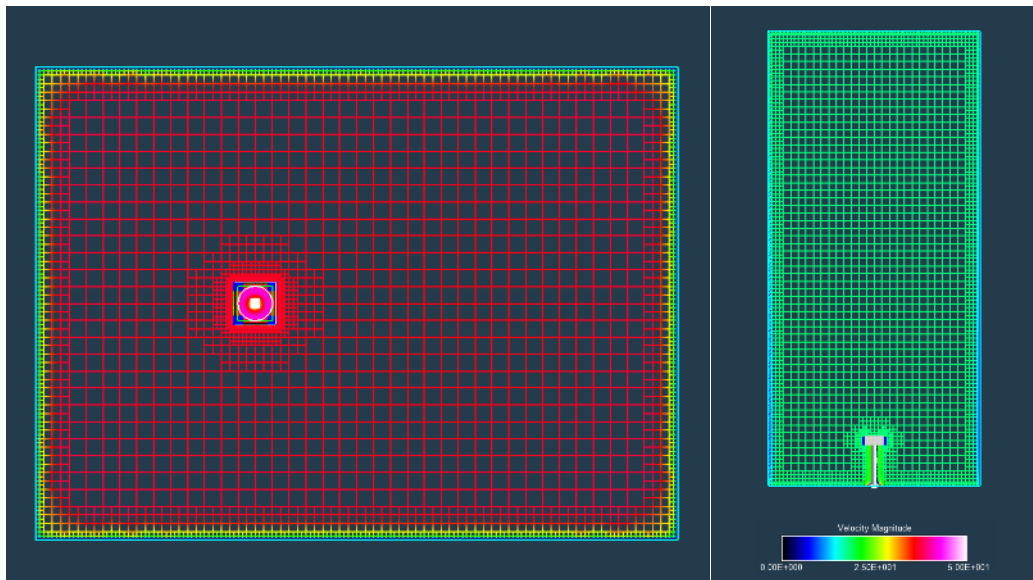


Figure C54. 14-mbar 1-Stack test 14 max velocity visualizations.

2-Stack:

Test 1: value does not line up with other data generated; much higher.

Test 2: value does not line up with other data generated; much higher.

Test 3: value does not line up with other data generated; much higher.

Test 4: solution diverged and was higher than anticipated.

Test 5:

Residual History

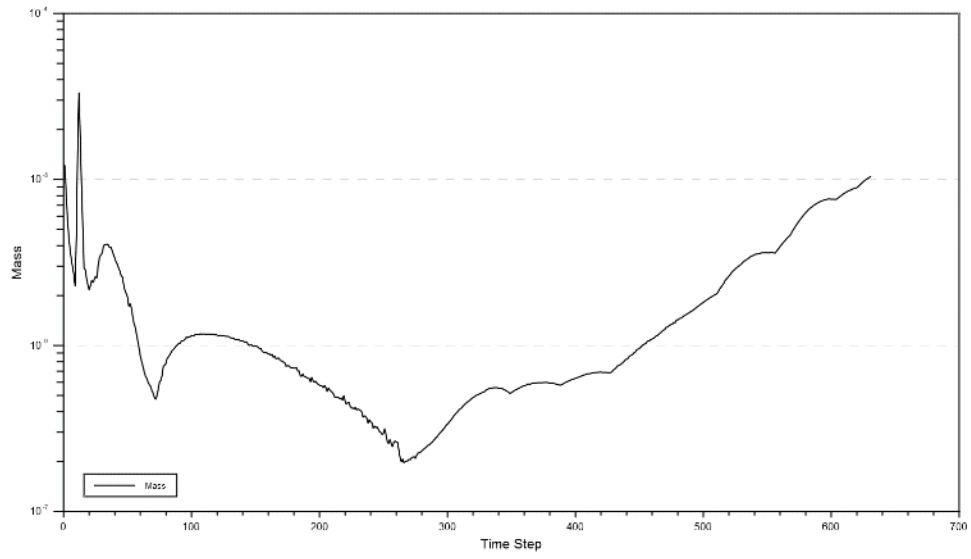


Figure C55. 14-mbar 2-Stack test 5 full residual.

Rotor Performance History

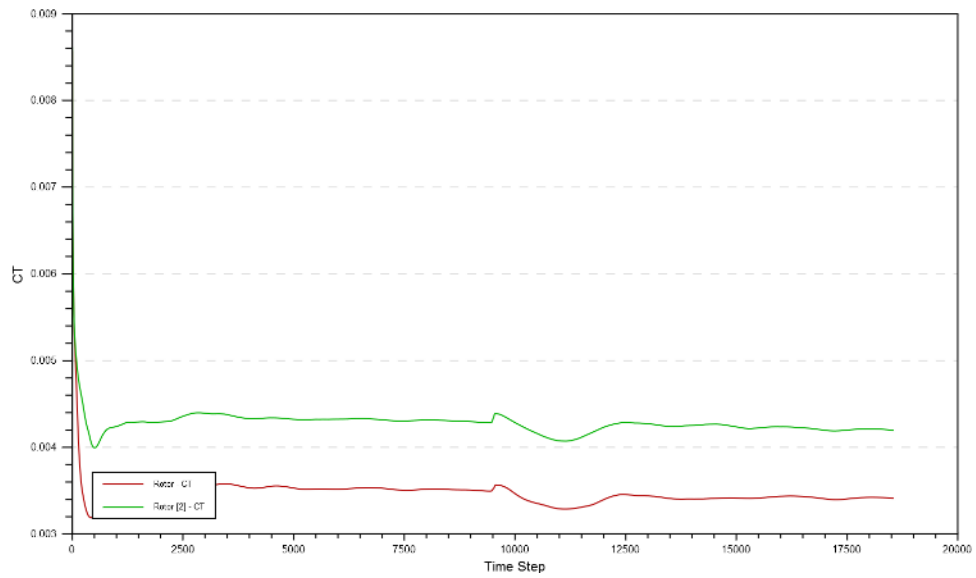


Figure C56. 14-mbar 2-Stack test 5 full CT.

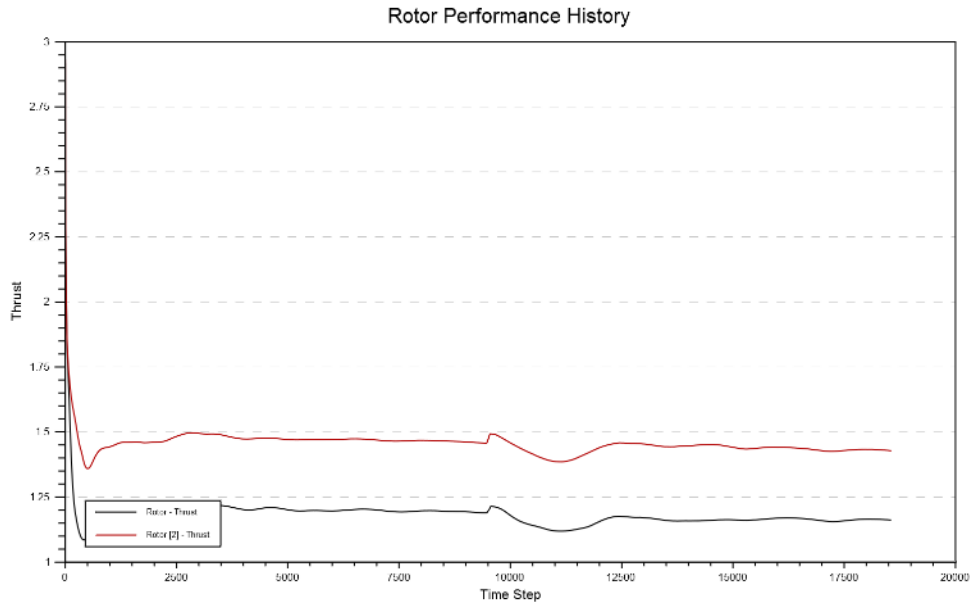


Figure C57. 14-mbar 2-Stack test 5 full thrust.

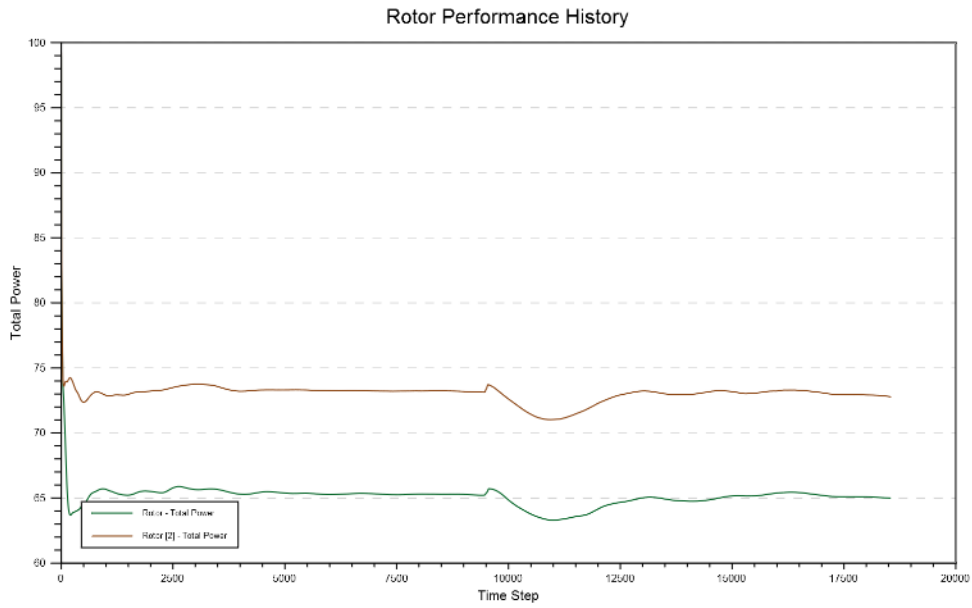


Figure C58. 14-mbar 2-Stack test 5 full total power.

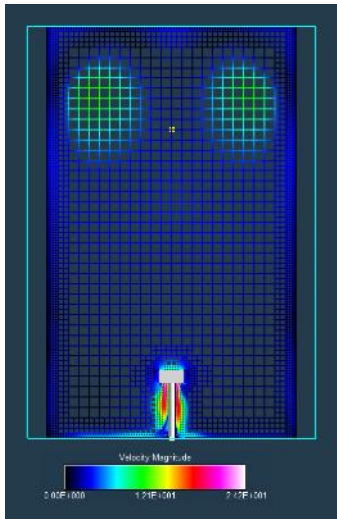


Figure C59. 14-mbar 2-Stack test 5 full velocity.

Test 6:

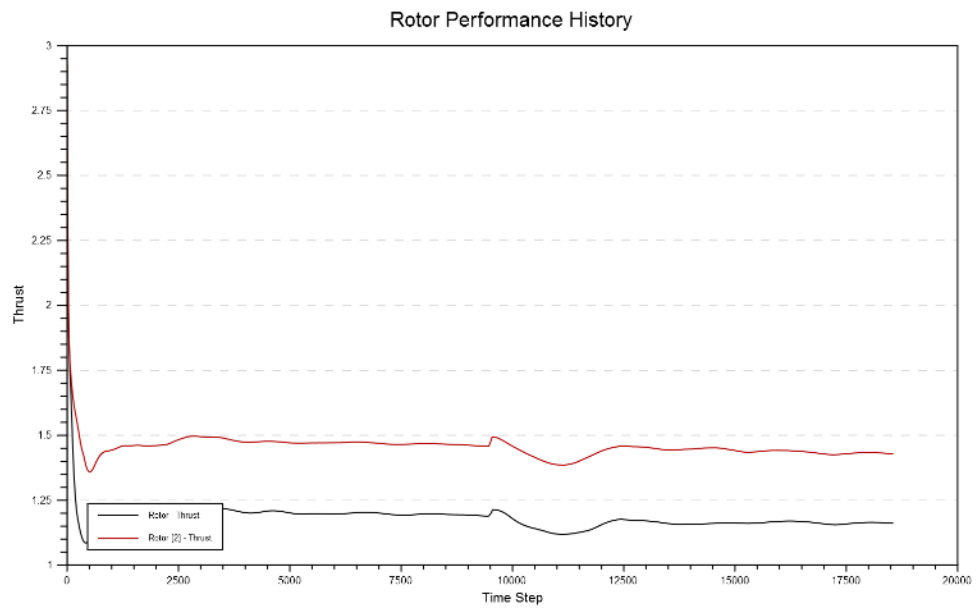


Figure C60. 14-mbar 2-Stack test 6 N242 thrust.

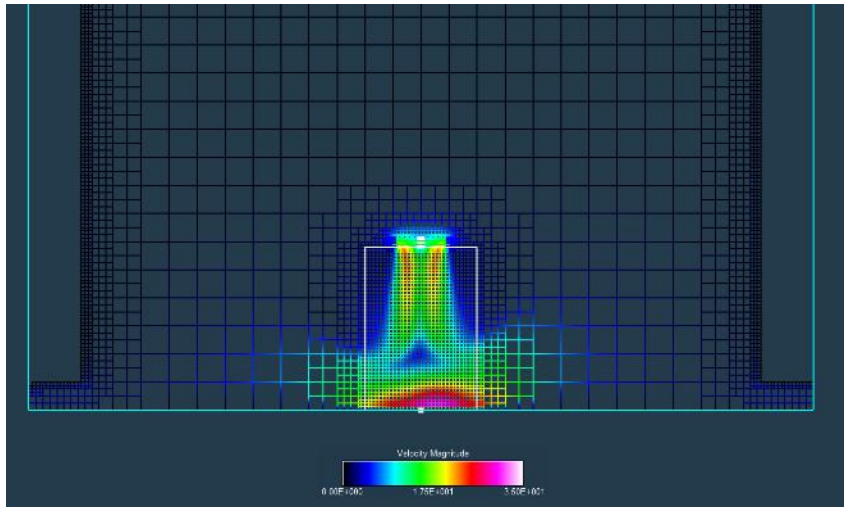


Figure C61. 14-mbar 2-Stack test 6 N242 velocity.

Test 7: bad velocity setup, failed to run.

Test 8:

Rotor Performance History

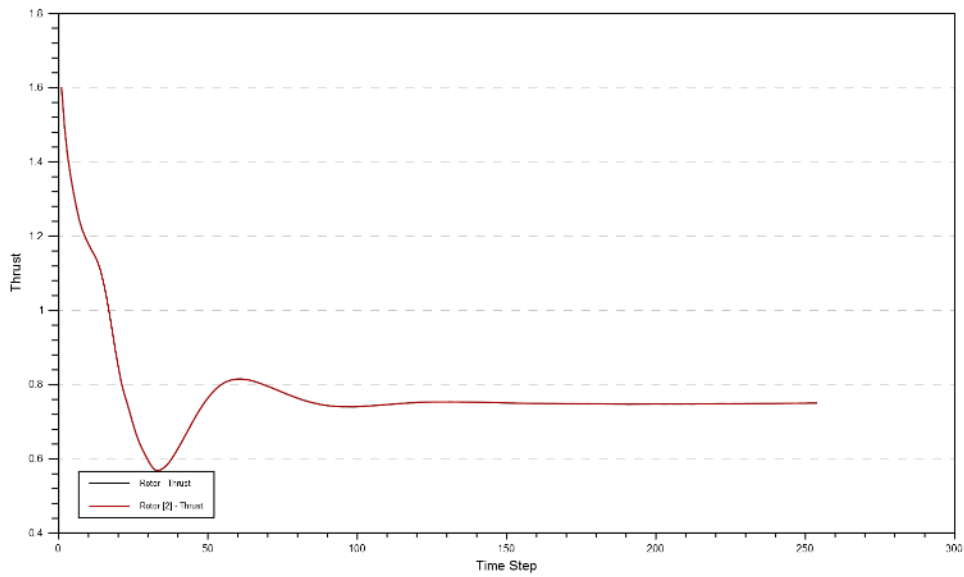


Figure C62. 14-mbar 2-Stack test 8 max velocity thrust.

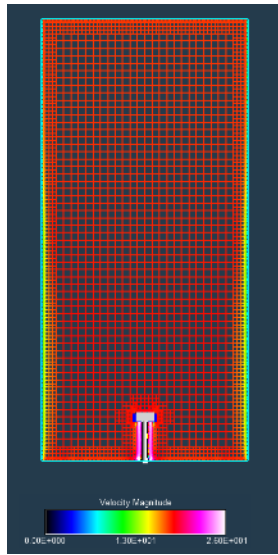


Figure C63. 14-mbar 2-Stack test 8 max velocity visualization.

Test 9:

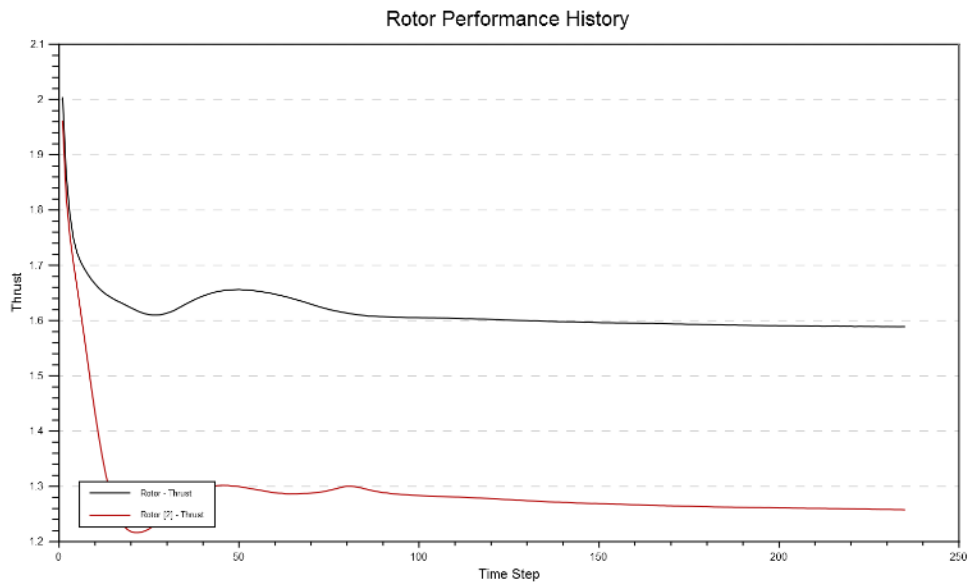


Figure C64. 14-mbar 2-Stack test 9 isol thrust.

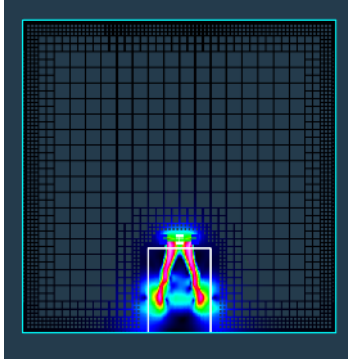


Figure C65. 14-mbar 2-Stack test 9 isol velocity.